National Defence / Défense nationale

TEMPORAL STATISTICS OF LOW-ANGLE GROUND CLUTTER (U)

by

H.C. Chan
Surface Radar Section
Radar Division

DEFENCE RESEARCH ESTABLISHMENT OTTAWA
REPORT NO. 1021

PCN
041LC12

December 1989
Ottawa

90-04045/

TEMPORAL STATISTICS OF LOW–ANGLE GROUND CLUTTER

ABSTRACT

Detailed knowledge of the temporal statistics of ground clutter is essential to determine the detection threshold settings so as to maximize the probability of target detection while maintaining an acceptable probability of false alarm. The performance of existing false alarm control schemes is often limited due to a lack of detailed knowledge of the ground clutter temporal statistics. In this study we analyze experimental data to characterize the temporal statistics of low–angle ground clutter in terms of the clutter's linear amplitude distribution. Effects of radar frequency, polarization, waveform resolution, land covers and wind speed on the statistics are examined.

The results show that the Ricean distribution and its limiting case, the Rayleigh distribution, are appropriate models for ground clutter in steady–state wind conditions. This implies that the diffuse clutter components, which give rise to the random properties of ground clutter may be modeled as a complex Gaussian process. We found, however, that at any given time there is a fraction of the resolution cells with clutter data having nonstationary temporal statistics not well modelled by the Ricean or Rayleigh distribution. The frequency of occurrence of nonstationary clutter statistics depends on radar frequency, land cover and wind speed. Forested land cover represents the worst case scenario. Application of the results of this study to determine optimal detection threshold settings is discussed.

Résumé

Une connaissance détaillée des statistiques temporelles des échos radar du sol est essentielle pour déterminer le réglage du seuil de détection, de façon á maximiser la probabilité de détection de la cible tout en maintenant une probabilité convenable de fausses alarmes. La performance des moyens existants pour le contrôle des fausses alarmes est souvent limitée à cause d'un manque de connaissance des statistiques temporelles du fouillis de sol. Dans cette étude nous avons analysé des données expérimentales pour caractériser les statistiques temporelles des échos du sol à des petits angles d'élévation en termes d'une distribution linéaire de l'amplitude du fouillis. Les effets de la fréquence du radar, de la polarisation, du pouvoir séparateur de la forme d'onde, du type de terrain et de la vitesse des vents sur les statistiques ont été examinés.

Les résultats ont montré que la distribution de Rice et à la limite, celle de Rayleigh, sont des modèles appropriés pour les échos du sol dans des conditions de vents stables. Ceci signifie que les composantes diffuses du fouillis, lesquelles donnent les propriétés aléatoires du fouillis de sol, peuvent être modelées par un processus gaussien complexe. Cependant, en pratique nous trouvons qu'à certains moments il y a une fraction des cellules de résolution qui ont des statistiques temporelles non stationnaires et qui, ne sont pas bien représentées par une distribution de Rice or de Rayleigh.. La fréquence à laquelle ces statistiques de fouillis non stationnaires apparaissent dépend de la fréquence du radar, du type de végétation et de la vitesse des vents. Les régions boisées représent le pire cas. Nous discutons l'application des résultats de cette étude pour déterminer l'établissement optimal du seuil de détection.

EXECUTIVE SUMMARY

Ground–based surveillance radars employ a variety of signal processors of varying degree of sophistication to combat ground clutter. One of the important performance requirements is false alarm rate regulation. In order to maximize the probability of target detection while maintaining an acceptable false alarm rate, the detection threshold setting must be determined optimally. This requires a detailed knowledge of the temporal statistics of clutter. The performance of existing false alarm control schemes is often limited due to a lack of this detailed knowledge.

In this study we analyze experimental data to characterize the temporal statistics of low–angle ground clutter in terms of the clutter's linear amplitude distribution. We examine the effects of radar frequency, polarization, waveform resolution, land covers and wind speed on the clutter statistics.

The results show that the Ricean distribution and its limiting case, the Rayleigh distribution, are appropriate models for ground clutter in steady–state wind conditions. This implies that the diffuse components, which give rise to the random properties of ground clutter approach a complex Gaussian process. We find, however, that at any given time there is a fraction of the resolution cells in a surveillance area with nonstationary statistics which are not well modelled by the Ricean or Rayleigh distribution. The frequency of occurrence of nonstationary clutter depends on radar frequency, land cover and wind speed. Forested land cover represents the worst case scenario.

We study in detail the nonstationary behaviour of ground–clutter amplitude and conclude that this nonstationarity is a result of sudden wind–speed changes. In cases where the clutter statistics are predominantly Ricean, the actual probability of false alarm plotted as a function of the detection threshold is bounded above by the theoretical curve of the Rayleigh model. In other instances, clutter processes which are predominantly Rayleigh could produce a false alarm rate exceeding that predicted by the Rayleigh model. We discuss the application of the results of this study in the determination of optimal detection threshold settings. For an optimum threshold setting, the predominant statistical type (Ricean or Rayleigh) of the clutter in each resolution cell should be monitored. The proper threshold setting is then determined according to the type, with a safety factor to account for nonstationary clutter behaviour.

TABLE OF CONTENTS

1. Introduction. 1

2. Low-angle ground clutter data and models for clutter amplitude statistics. 1

   2.1 Low-angle ground clutter data. 1

      2.1.1 The MIT Lincoln Laboratory Phase I data. 2
      2.1.2 The DREO S-band experimental phased array radar. 2

   2.2 Models for clutter-amplitude statistics. 3

      2.2.1 The Ricean model. 3
      2.2.2 The Rayleigh model. 6

   2.3 Parameter estimation for the Ricean model. 7

3. Experimental observation of temporal ground-clutter statistics. 8

   3.1 Statistical classification of Phase I clutter data. 8

   3.2 Statistical classification of DREO clutter data. 20

   3.3 Nonstationary clutter processes. 21

4. Conclusions 29

   4.1 Summary of results. 29

   4.2 Constant false-alarm rate considerations. 32

      4.2.1 Optimal detection threshold. 33
      4.2.2 Detection threshold for nonstationary clutter processes. 34

5. References. 34

6. Acknowledgement. 35

LIST OF FIGURES

Figure 1. A typical example of X-band ground clutter:
(a) Amplitude-phase scatter plot;
(b) Amplitude histogram. 4

Figure 2. A plot of parameter β as a function of parameter y. 8

Figure 3. Comparison of a weakly Ricean process with a Rayleigh process: (a) Probability density function;
(b) Probability of false alarm..... 12

Figure 4. An example of clutter processes fitting the Ricean model
(a) Histogram
(b) Probability of false alarm. 13

Figure 5. An example of a clutter process with poor visual fit to a Ricean model but with an acceptable P_{fa} vs. V_T match:
(a) Histogram; (b) Probability of false alarm..... 14

Figure 6. P_{fa} vs V_T curves of a clutter process fitting the Rayleigh model. 15

Figure 7. An example of non-stationary clutter processes:
(a) amplitude-phase scatter plot; 15
(b) Histogram; 16
(c) Probability of false alarm. 16

Figure 8. In-phase waveform of a nonstationary clutter process with a predominantly Ricean fit. 22

Figure 9. Example of a nonstationary clutter process with a predominantly Ricean fit:
(a) Histogram;
(b) Probability of false alarm. 24

Figure 10. In-phase waveform of a nonstionary clutter process with a predominantly Rayleigh fit. 25

Figure 11. An example of nonstationary clutter processes with a predominantly Rayleigh fit:
(a) Histogram;
(b) Probability of false alarm. 26

Figure 12. Distribution of parameter β for clutter in urban areas at the DREO site. 27

Figure 13. Distribution of parameter β for clutter in agricultural areas at the DREO site. 28

Figure 14. Distribution of parameter β for clutter in forested areas at the DREO site. 30

1. Introduction.

The performance of ground–based surveillance radars in areas within the radar horizon is largely clutter–limited. Modern signal processing techniques such as moving target indicator (MTI) filtering and Doppler processing have improved the detection of moving targets to a level that is near–optimum. However, for targets with very low radial velocities, the detection performance is very much dependent on the magnitude and the temporal statistics of the clutter returns.

The temporal statistics of ground clutter describe the statistical variation of the ground clutter magnitude over time for a given resolution cell. Knowledge of these statistics is necessary to establish the probability of false alarm for a given threshold setting. Conversely, a lack of this knowledge could cause one to over estimate the threshold setting with a consequent loss in the probability of detection.

An analysis of low–angle ground clutter data indicated that ground clutter comprises several spectral components resulting from the scattering of the radar signal by fixed objects and objects set in motion by wind. Since wind–induced movement of objects is stochastic, the amplitude of ground clutter is also a random process. The intrinsic statistics and the relative proportion of the individual components determine the random characteristics of the composite clutter.

The most commonly adopted models for describing ground clutter amplitude statistics are the Rayleigh and Ricean Distributions. These models can be shown to have a physical basis. In this report, we estimate the amplitude statistics of low–angle ground clutter by analyzing data collected by the MIT Lincoln Laboratory's Phase I mobile radar facility [1] and the DREO S–band phased–array radar.

Section 2 briefly describes the data base and the Ricean and Rayleigh models. Section 3 presents the analysis of the amplitude statistics of low–angle ground clutter at various frequency bands. The effects of wind speed, radar frequency, resolution and land cover on clutter temporal statistics are examined. Section 4 summarizes the analysis results and discusses these in terms of detection and false alarm rate performance improvement.

2. Low–angle ground–clutter data and models for clutter–amplitude statistics.

2.1 Low–angle ground–clutter data.

A random process may either be stationary (one whose statistics are not affected by a shift in time origin) or nonstationary. In general, ground clutter is not a stationary random process because the underlying mechanism (wind) which produces the randomness of ground clutter could be nonstationary over an extended period of time. The wind field observed in a given area is time–varying and unpredictable. However, for a finite period of time in which the wind velocity attains a steady–state condition, the observed ground clutter may be considered to be stationary. A different set of model parameters must be determined for each wind condition as the statistics of the clutter change significantly.

To obtain accurate statistical information, ground clutter must be observed over a sufficiently long period of time. The length of an appropriate observation period depends on how often the wind speed and direction changes. For the purpose of characterizing

amplitude statistics using experimental data, a more practical constraint is the length of the recorded data. In this section we describe the two data sources used to obtain the amplitude statistics of ground clutter. Their advantages and weaknesses are discussed.

2.1.1 The MIT Lincoln Laboratory Phase I data

The MIT Lincoln Laboratory's Phase I ground–clutter data base comprises coherent data collected for five frequencies (X–, S–, L–, U– and V–bands), with dual polarization (Vertical transmit/Vertical receive and Horizontal transmit/Horizontal receive) and with three range resolutions (15m, 36m and 150m). These data were collected at a variety of Canadian and American sites. Details of this data base may be found in [1]. Data suitable for the characterization of ground–clutter amplitude statistics must span a sufficiently long time interval. Hence a stationary antenna must be employed in the collection of the data. There was a small amount of Phase I data collected in selected sites which employed a stationary antenna and a relatively long dwell time, typically 20 seconds to one minute. These data were of a type that allowed an examination of the effects of radar frequency, resolution and polarization on clutter statistics. However, the (i) quantity of data, (ii) range of observed wind velocity and (iii) variety of land cover types are inadequate for reliable compilation of the statistical effects sought. In particular, there was not enough variation in land cover type to examine the relative frequency of occurrence of each statistical model in various land covers. These limitations came about because the primary purpose of PHASE I was to collect spatial statistics of ground clutter which required a large ensemble of relatively short–time averages of the clutter magnitude from individual resolution cells. Consequently, long–dwell data collection was only performed occasionally in order to minimize the magnetic–tape storage requirement.

2.1.2 The DREO S–band experimental phased array radar.

The Defence Research Establishment Ottawa (DREO) Radar Division's S–band coherent phased array radar facility was used to collect ground clutter data which were suitable for a detailed statistical analysis. This system allows the use of very long dwells in any selected azimuthal direction within the field of view which is essential for the estimation of temporal statistics. For data collection, we used a radar dwell of 30720 pulses at a PRF of 100 Hz. This particular combination of PRF and number of pulses gave a 307.2–second observation period, long enough to characterize a stationary random process. The limitation of the DREO radar is that it is a single–band/single–polarization radar. The essential characteristics of the DREO S–band radar are summarized in Table I

Table I. Characters of the DREO Radar Division S–band Phased Array Radar.

Frequency	2970 MHz
Polarization	Horizontal
Pulse Width	1 μs
PRF	100 Hz
Peak Power	2.5 kW
Azimuthal Beamwidth	4°

2.2 Models for clutter–amplitude statistics.

Clutter statistics can be characterized in terms of the probability distribution for either the linear amplitude or the squared–magnitude. The coherent clutter samples used in this analysis were taken at the I– and Q–channel analog–to–digital converters (ADC). One can obtain either the envelope or the squared–magnitude of the clutter samples from the coherent clutter time series by using Eqn(1):

$$a_i = (x_i^2 + y_i^2)^{\frac{1}{2}} \tag{1}$$

for the linear amplitude and Eqn (2):

$$a_i^2 = x_i^2 + y_i^2 \tag{2}$$

for the squared–magnitude, where

x_i, and y_i, i=1,2,...,N are the amplitudes of the I– and the Q–components respectively.

The probability density function (pdf) of the ground–clutter amplitude was used to characterize the statistics of the clutter in each resolution cell. Practically the pdf may be approximated by the histogram of the clutter samples. We chose to use the linear amplitude because of dynamic range consideration in forming the histograms, since the squared–magnitude would span a wider dynamic range than the linear amplitude.

Figure 1a shows a typical amplitude–phase scatter plot of an X–band, V–Pol clutter time series over a period of 1 minute. The amplitude–phase scatter plot captures the history or the "foot–print" of the instantaneous clutter amplitude on the phase plane over a finite time interval. The histogram (Figure 1b) was obtained by first dividing the portion of the phase plane, which extends from the origin to a radius encompassing the largest clutter sample, into a number of equal–width concentric rings (bins). Secondly, the number of clutter amplitudes which were within each bin was recorded. Finally the histogram (the probability that the clutter amplitude falls within a particular bin) was obtained by dividing the counts in each bin by the total number of clutter samples in the time series.

2.2.1 The Ricean Model

The Ricean probability density function, derived by Rice [2] from the analysis of the statistical properties of a sine wave in additive noise, is given by:

$$p(z) = \frac{z}{\sigma^2} \exp\{-\frac{A^2+z^2}{2\sigma^2}\} I_0\left[\frac{2Az}{2\sigma^2}\right] \tag{3}$$

where A is the amplitude of the sine wave,
z is the envelope of a complex Gaussian noise process with standard deviation σ;
and $I_0(z)$ is the modified Bessel function of the first kind of order zero.

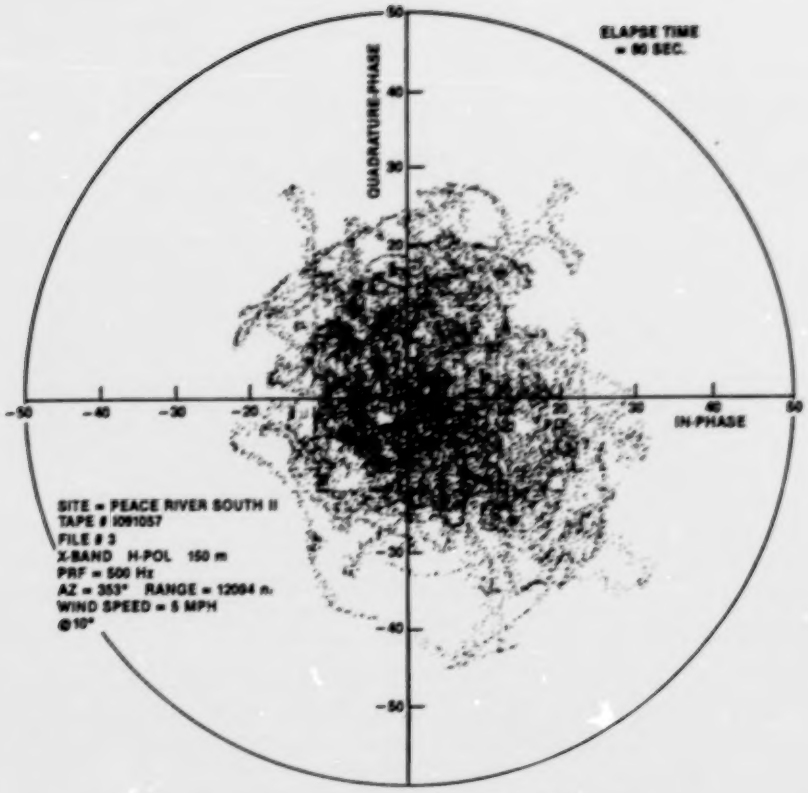

(a) Amplitude–phase scatter plot

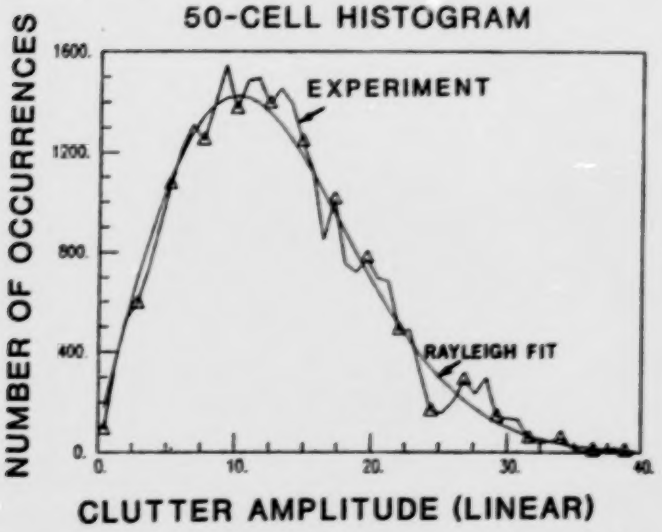

(b) Histogram

Figure 1. An example of X–band ground clutter.

The first and second moments of a Ricean process are given by [2]:

$$\langle z \rangle = \left[\frac{\pi}{2}\right]^{\frac{1}{2}} \sigma \exp\left[-\frac{A^2}{4\sigma^2}\right] \left[\left[1+\frac{A^2}{2\sigma^2}\right] I_0\left[\frac{A^2}{4\sigma^2}\right] + \frac{A^2}{2\sigma^2} I_1\left[\frac{A^2}{4\sigma^2}\right]\right] \quad (4)$$

and

$$\langle z^2 \rangle = A^2 + 2\sigma^2 \quad (5)$$

respectively, where

$I_1(x)$ is the modified Bessel function of the first kind of order 1.

In many respects ground clutter has similar attributes as those of a sine wave in additive noise. Analysis of radar ground clutter indicated that ground clutter generally comprises a coherent component and one or more diffuse components. The coherent component is essentially a constant or a slow–varying signal and, for practical purposes, can be considered as a sine wave with zero frequency. The receiver noise is known to have Gaussian statistics. If the statistics of the diffuse components are describable by complex Gaussian distributions, then the composite of the coherent component, the diffuse components and receiver noise should have a Ricean distribution.

There are some theoretical arguments which can be put forward to support such a model. It is well known that a Gaussian random process may be obtained by summing a large number of random numbers. This is known as the central limit theorem [3]. These random numbers may have different distribution densities. The echo from a given resolution cell is the coherent sum of the signal scattered back to the radar by individual objects such as buildings, crops and trees that are within the confines of the resolution cell. Returns from immovable objects constitute the coherent component. The diffuse components are returns from the ensemble of movable objects such as tree leaves and branches. Since the dimension of the resolution cell is large compared to the wavelength for surveillance radars, there are numerous movable objects inside a resolution cells which contribute to the diffuse components.

If a coherent pulse train is transmitted by the radar at a certain pulse repetition interval (PRI), the echoes of individual pulses would vary randomly because the wind causes individual scatterers to assume a slightly different position and orientation from pulse to pulse. As a result, the amplitude and phase of the echoes from individual scatterers will be different from pulse to pulse. This is equivalent to drawing a new random number from each distribution and summing them together. One therefore expects that the diffuse component would be a complex Gaussian process.

For target detection, a threshold value V_T is set for each resolution cell according to the clutter statistics. For a clutter process fitting a Ricean distribution, the probability of false alarm (P_{fa}) is obtained by integrating Eqn(3) from the threshold V_T to infinity. To determine the appropriate threshold setting for a Ricean clutter process, both parameters A and σ^2 must be estimated. These are calculated from the first and second moments.

2.2.2 The Rayleigh model.

The Rayleigh distribution is a limiting case of the Ricean distribution. If parameter A in Eqn (4) is set to zero, the Rayleigh pdf results:

$$p(z) = \frac{z}{\sigma^2} \exp\{-\frac{z^2}{2\sigma^2}\} \tag{6}$$

The first and second moments of the Rayleigh distribution are:

$$\langle z \rangle = \left[\frac{\pi}{2}\right]^{1/2} \sigma \tag{7}$$

and

$$\langle z^2 \rangle = 2\sigma^2 \tag{8}$$

respectively.

A Rayleigh random process requires only one parameter, σ, for its characterization. Hence it is attractive from the standpoint of determining the proper threshold setting for a specified P_{fa}. The P_{fa} of a Rayleigh clutter process for a threshold setting of V_T is obtained from Eqn(6):

$$\begin{aligned} P_{fa} &= \int_{V_T}^{\infty} \frac{z}{\sigma^2} \exp\{-\frac{z^2}{2\sigma^2}\}\, dz \\ &= \exp\{-\frac{V_T^2}{2\sigma^2}\} \end{aligned} \tag{9}$$

Since parameter σ is related to the mean of the Rayleigh process through Eqn(7), the required threshold setting may be conveniently found by multiplying the mean value by a scalar which is a function of the P_{fa} only. For a given a probability of false alarm, the required V_T is determined from Equations (7) and (9):

$$V_T = \sqrt{-2\sigma^2(\ell n\, P_{fa})} = k \langle z \rangle \tag{10}$$

where $k = [-\frac{4}{\pi}(\ell n\, P_{fa})]^{\frac{1}{2}}$

The appropriateness of the Ricean and Rayleigh models in describing the amplitude statistics of low–angle ground clutter will be verified by experimental observation. This is done in section 3.

2.3 Estimation of parameters for the Ricean model.

As discussed in Section 2.1, the determination of the detection threshold setting for a Ricean clutter process requires the knowledge of parameters A and σ^2. Dividing both sides of Eqn (5) by $2\sigma^2$ yields:

$$y = \frac{\langle z^2 \rangle}{2\sigma^2} = \frac{A^2}{2\sigma^2} + 1 \tag{11}$$

Substitution of Eqn (11) into Eqn (4) yields:

$$\langle z \rangle = \left[\frac{\pi}{2}\right]^{1/2} \sigma \exp\left[-\frac{(y-1)}{2}\right] \left[y\, I_0\left(\frac{y-1}{2}\right) + (y-1)\, I_1\left(\frac{y-1}{2}\right)\right] \tag{12}$$

We define parameter β as the ratio between the squared first moment and the second moment. From Eqns (4), (11) and (12) we have:

$$\beta = \frac{\langle z \rangle^2}{\langle z^2 \rangle} = \frac{\pi \exp[-(y-1)] \left[y\, I_0\left(\frac{y-1}{2}\right) + (y-1)\, I_1\left(\frac{y-1}{2}\right)\right]^2}{4y} \tag{13}$$

A plot of β as a function of y is shown in Figure 2. A value of y = 1 represents the limiting case for a Rayleigh process (A=0). In this case $\beta=\pi/4$. On the other hand, as y approaches infinity, β approaches unity. This represents the case of a large coherent component or a diminishingly small diffuse component.

The value of y can be obtained from Eqn (13) using numerical techniques such as the Newton's method [4], after computing β from the sample first and second moments. From y, one can obtain the threshold setting, V_T, for a given P_{fa}. In a practical radar, the pre–computed threshold settings can be stored in a look–up table in terms of β. Parameters A and σ are obtained from:

$$2\sigma^2 = \frac{\langle z^2 \rangle}{y} \tag{14}$$

and

$$A^2 = \langle z^2 \rangle \frac{y-1}{y} \tag{15}$$

respectively.

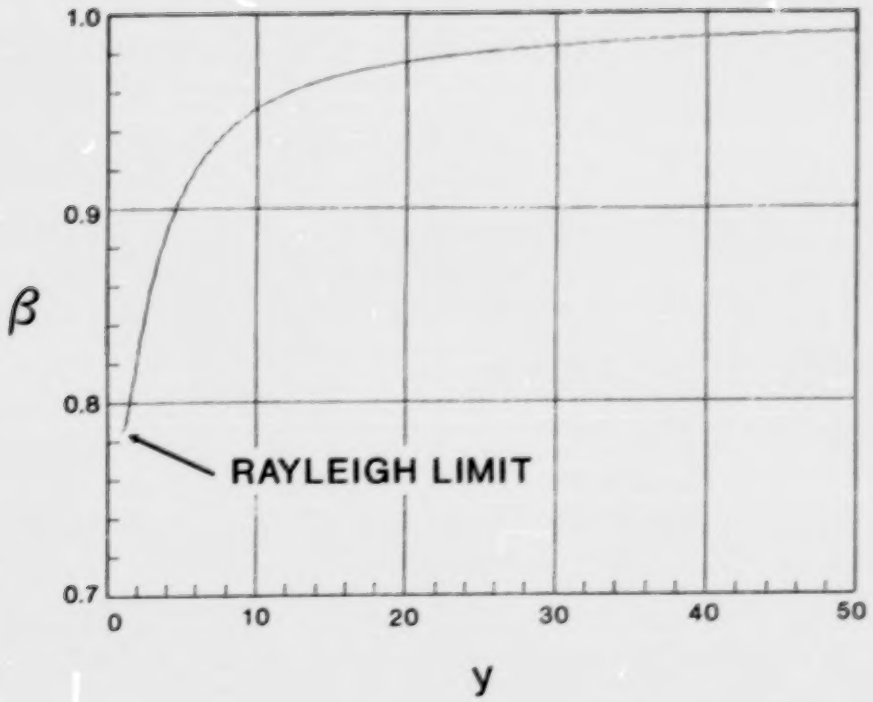

Figure 2. Parameter β as a function of y.

3. Experimental observation of temporal ground–clutter statistics.

3.1 Statistical classification of Phase I clutter data.

Although the Rayleigh model is a special case of the Ricean model, we shall compare the clutter data against the two models separately for the following reasons. Firstly, conventional radar signal processors such as noncoherent clutter maps store only the sample mean of the clutter. To determine the detection threshold from the mean, one implicitly assumes that the clutter statistics are completely determined by its first moment. The Rayleigh distribution fits this requirement. Secondly, we would like to examine how often ground clutter statistics approach that of a Rayleigh model.

Long–dwell pulse–by–pulse data from Beiseker, Picture Butte and Peace River South II, Alberta were analyzed. The histograms of the clutter time series were computed and compared to both models. In each of these three sites, data were collected in a range interval of about 2 km for a selected azimuthal direction. For the low resolution waveform (150m), data from 16 resolution cells were available. For the high resolution waveform (15m for X–, S– and L–bands, 36m for UHF and VHF), data from 76 resolution cells were recorded. The characteristics of these data are summarized in Table II.

Table II. Phase I data used in amplitude statistics analysis

(a) Site Beiseker	Band	Tape No.	File No.	Az	Range Start (km)	PRF (Hz)	Wind Speed (mph)	Dwell (No. of pulses)
Low Resol. (150m)	X	I018351	4	160°	11.5	1000	7	10240
	S	I018325	3	160°	13.5	1000	7	10240
	L	I018351	2	160°	13.5	1000	7	10240
	U	I018337	2	160°	13.5	1000	7	10240
	V	I018316	7	160°	13.5	1000	7	10240
High Resol. (X,S,L 15m) (U,V 36m)	X	I018356	1	160°	12.0	1000	7	10240
	S	I018326	1	160°	14.0	1000	12	10240
	L	I018340	3	160°	13.5	1000	7	10240
	U	I018340	1	160°	13.5	1000	7	10240
	V	I018317	2	160°	13.5	1000	5	10240

(b) Site: Picture Butte: Az.=177° Range Start=23.0km PRF=500 Hz. Dwell=10240 pulses

		(V-POL)			(H-POL)		
	Band	Tape No.	File No.	Wind Speed (mph)	Tape No.	File No.	Wind Speed (mph)
Low Resol.	S	I021026	1	15	I021025	1	16
	L	I021007	1	11	I021007	2	11
	U	I021005	3	10	I021006	3	7
	V	I021030	3	7	I021033	1	7
High Resol.	S	I021008	3	15	I021018	5	16
	L	I021006	6	11	I021008	1	15
	U	I021005	2	10	I021006	2	7
	V	I021031	1	7	I021032	3	7

Table II: Phase I data used in amplitude statistics analysis (Cont'd)

(c) Site: Peace River South II: Az.=353°, Range Start=12 km
PRF=500 Hz. Dwell=30720 pulses

		(V-POL)			(H-POL)		
	Band	Tape No.	File No.	Wind Speed (mph)	Tape No.	File No.	Wind Speed (mph)
Low Resol.	X	I091056	1	5	I091057	3	5
	S	I091033	3	2	I091034	5	2
	L	I091029	2	8	I091030	3	8
	U	I091031	1	8	I091032	1	8
	V	I091005	2	5	I091006	2	1
High Resol.	X	I091054	2	5	I091056	2	5
	S	I091032	2	2	I091033	1	2
	L	I091028	2	8	I091029	3	8
	U	I091030	1	8	I091032	2	2
	V	I091005	1	1	I091006	1	1

Tests for goodness of fit [5], [6] of random data to statistical models are available to determine the relative merits of models. However, in this case, a visual fitting method was used, because (i) the small quantity of data made this practical and (ii) valuable physical insights were obtained by using the visual approach.

With regard to (ii) it is shown in what follows that, even though the fit of a Ricean distribution to the data was not exceptionally good in some cases, the use of a Ricean model produced an acceptably accurate estimation of the probability of false alarm. From a radar signal–processing point of view, these distributions are only of use for setting detection thresholds so as to achieve the specified probability of false alarm. That is, even though the fit may not have been good from a statistical point of view, the use of the model produced acceptable results.

We introduce the term "predominantly Rayleigh" to describe a clutter process which possesses attributes that are Rayleigh–like. These are (i) a β value that is close to to $\pi/4$ and (ii) a P_{fa} characteristic that is closer to that of a Rayleigh model than that of a Ricean model.

Similarly we use the term "predominantly Ricean" to describe a clutter process which has (i) a β value that is closer to unity than to $\pi/4$ and (ii) a P_{fa} characteristic that is closer to that of a Ricean model than that of a Rayleigh model.

Consider a Ricean process with a first moment $\langle z \rangle = 1$ and a value of $\beta = 0.8$. From Eqns (11), (12) and (13) we obtain the following parameter values for the Ricean model: $y = 1.5$, $A = 0.6455$ and $2\sigma^2 = 0.8333$. If one wants to approximate this process by a Rayleigh process, one computes the Rayleigh parameter σ from Eqn (7) and obtains a value of $\sigma_r = 0.79788$. Using these values, the pdf's and the P_{fa} characteristic of the Ricean process and its Rayleigh approximation are plotted in Figure 3a and 3b, respectively.

It can be seen that the two pdf's are very close, and the P_{fa} characteristics predicted by the Rayleigh approximation is only slightly worse than that calculated from the correct (Ricean) model. For example, at a P_{fa} of 10^{-5}, a threshold setting of $V_T = 3.83$ is required for a Rayleigh model, while a value of $V_T = 3.5$ is calculated for the Ricean model. In subsequent discussions, we shall classify a clutter process to be predominantly Rayleigh if the value of β is less than 0.8, and the P_{fa} characteristic is close to that of the Rayleigh model.

We have also observed clutter data with a P_{fa} characteristic which deviates significantly from those of the Rayleigh or the Ricean model. We found that these data resulted from short periods of change of clutter statistics most probably because of sudden wind–velocity changes. We shall call these clutter processes "nonstationary".

In the following, the frequency of occurrence of clutter data fitting the Rayleigh and Ricean models is tabulated for experiments performed in Beiseker, Picture Butte and Peace River South II, Alberta.

Before presenting the tables, several histograms and the corresponding probability of false alarm curves are shown in order to give some qualitative indication of how the data were classified. In Figure 4a is shown an amplitude histogram of a clutter time series from Peace River South II. The experimental parameters are listed on the figure. Superimposed is the Ricean density function calculated from the data. As can be seen, the fit was excellent. Figure 4b shows the probability of false alarm as a function of threshold setting for this data set. The theoretical P_{fa} curves for both the Ricean and Rayleigh models are superimposed. The P_{fa} vs V_T curve follows that of the Ricean model closely. For some data sets, the fit is less good, such as the one whose histogram is shown in Figure 5a. Nevertheless, the probability of false alarm curve for this data set still matches that predicted by the Ricean model. Figure 5b shows the corresponding P_{fa} vs V_T curve for this data set. Even though the histogram deviates substantially from the Ricean pdf, the false alarm behaviour in the low P_{fa} region follows that of the Ricean model very well.

An example of a clutter time series fitting the Rayleigh model is shown in Figure 1b. The corresponding P_{fa} vs V_T curves are shown in Figure 6. In this case, the theoretical P_{fa} curve for the Ricean model coincides with that of the Rayleigh model as predicted by theory.

We found some resolution cells where the clutter time series did not fit either the Ricean or the Rayleigh model. Figure 7 represents one example. In Figure 7a is shown the amplitude–phase scatter–plot of an S–band time series. The clutter samples form a number of clusters having distinct mean values at different times, as can be seen from the histogram in Figure 7b. The P_{fa} vs V_T curves for this data set is shown in Figure 7c. The P_{fa} behaviour is substantially different from the theoretical curves of both models in the low P_{fa} regions. Clutter processes with histograms similar to the above will be classified as "others" or nonstationary.

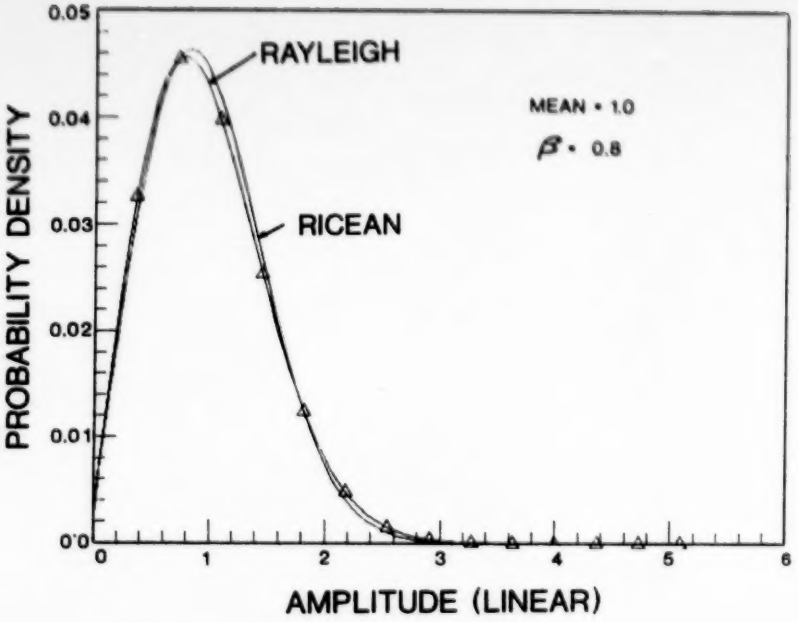

(a) Probability density function.

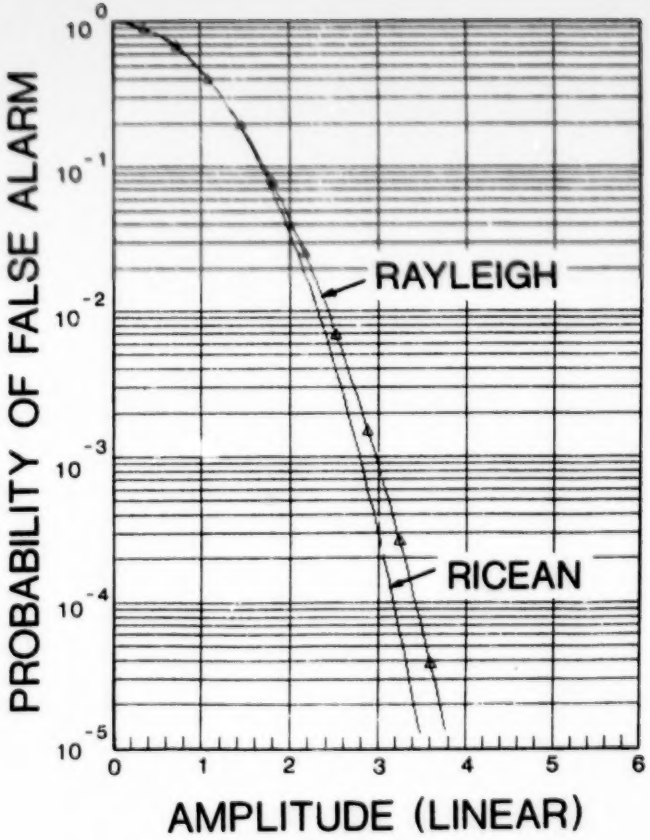

(b) Probability of false alarm.

Figure 3. Comparison of a weakly Ricean process with a Rayleigh process.

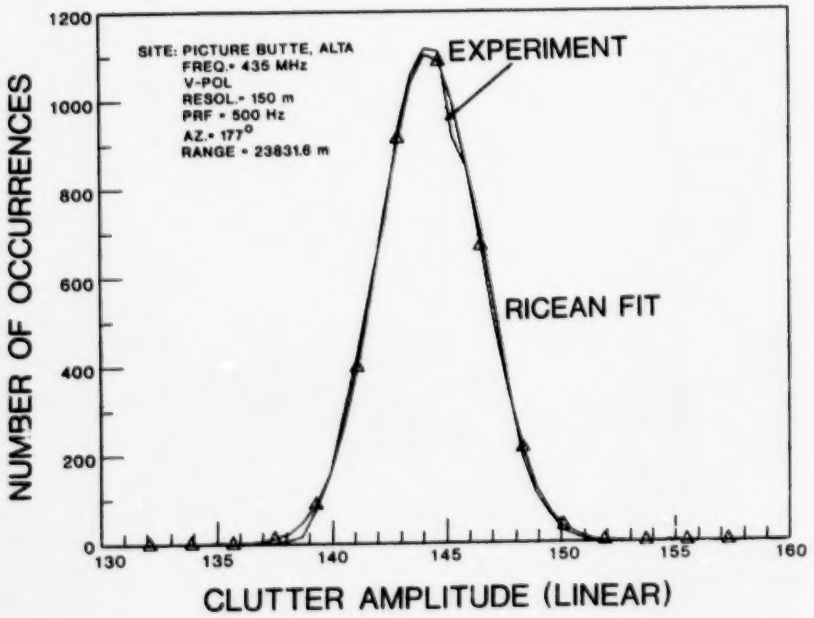

(a) Histogram.

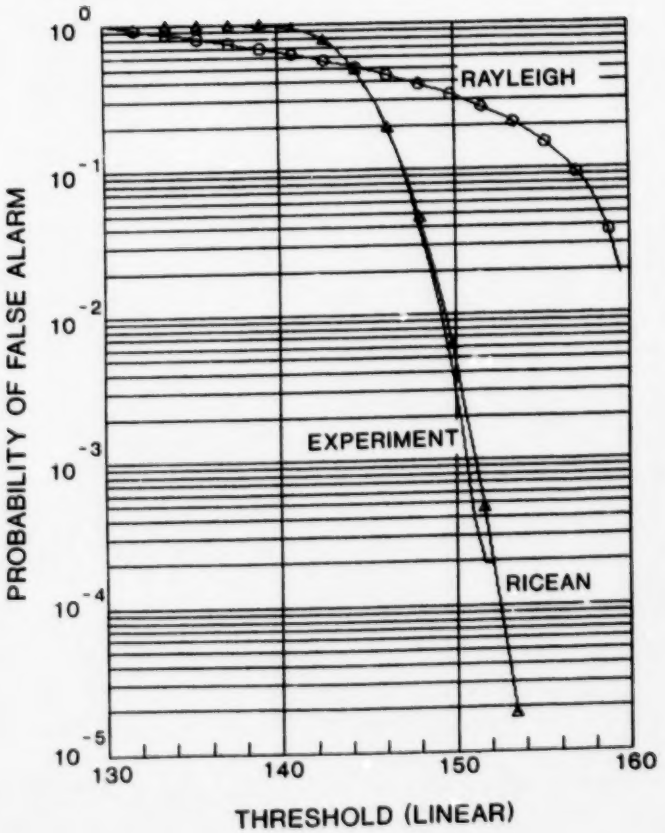

(b) Probability of false alarm.

Figure 4. An example of clutter processes fitting a Ricean model.

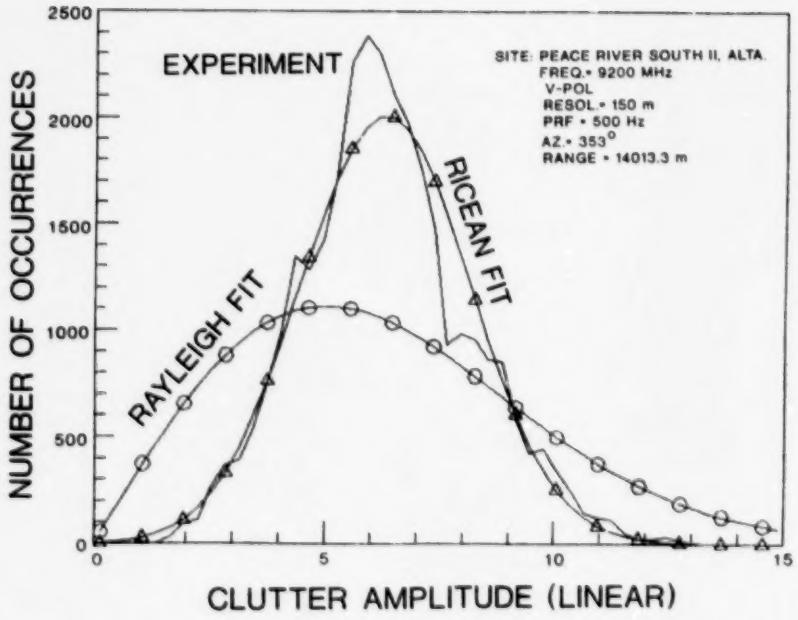

(a) Histogram.

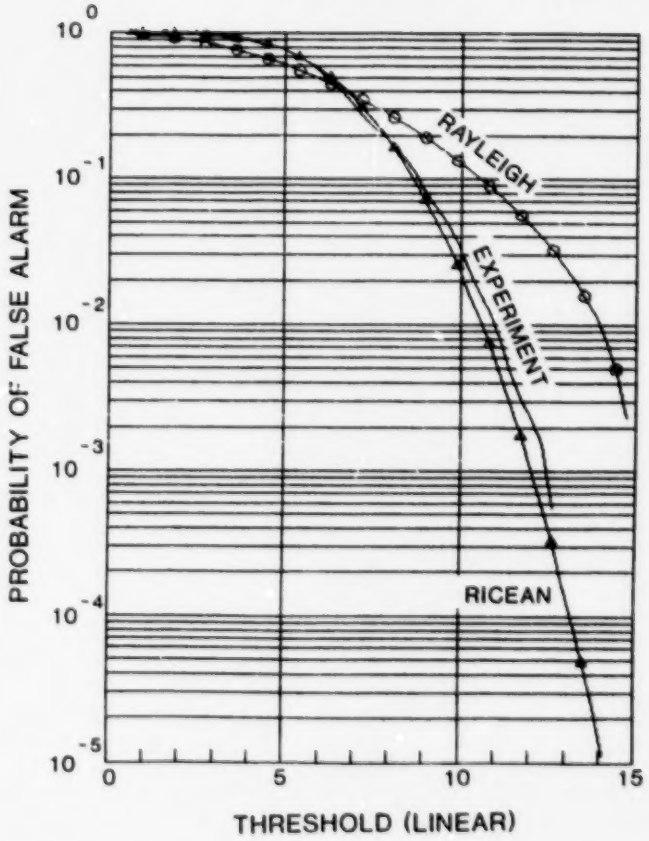

(b) Probability of false alarm.

Figure 5. An example of a clutter process with poor fit to a Ricean model but with an acceptable P_{fa} vs V_T match.

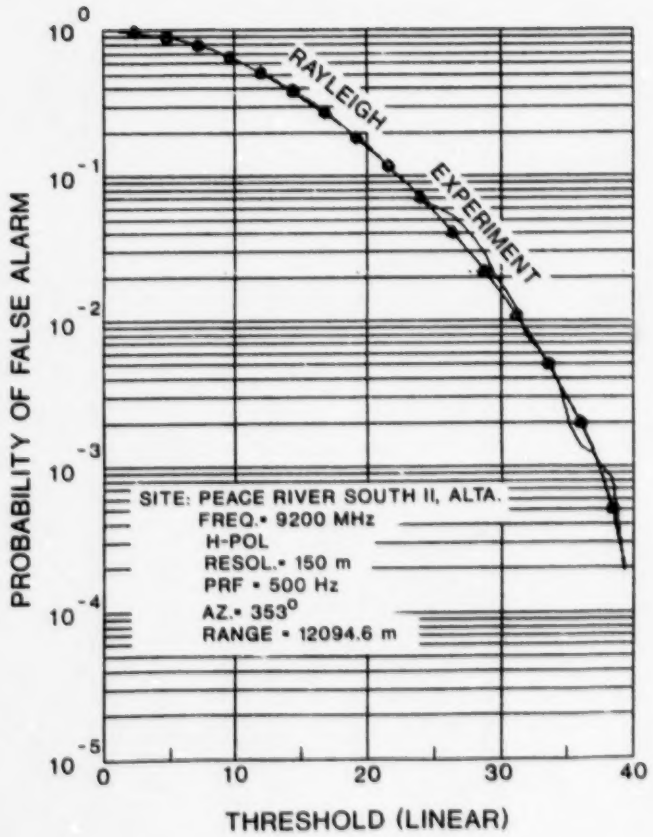

Figure 6. P_{fa} vs V_T curves of a clutter process fitting the Rayleigh model.

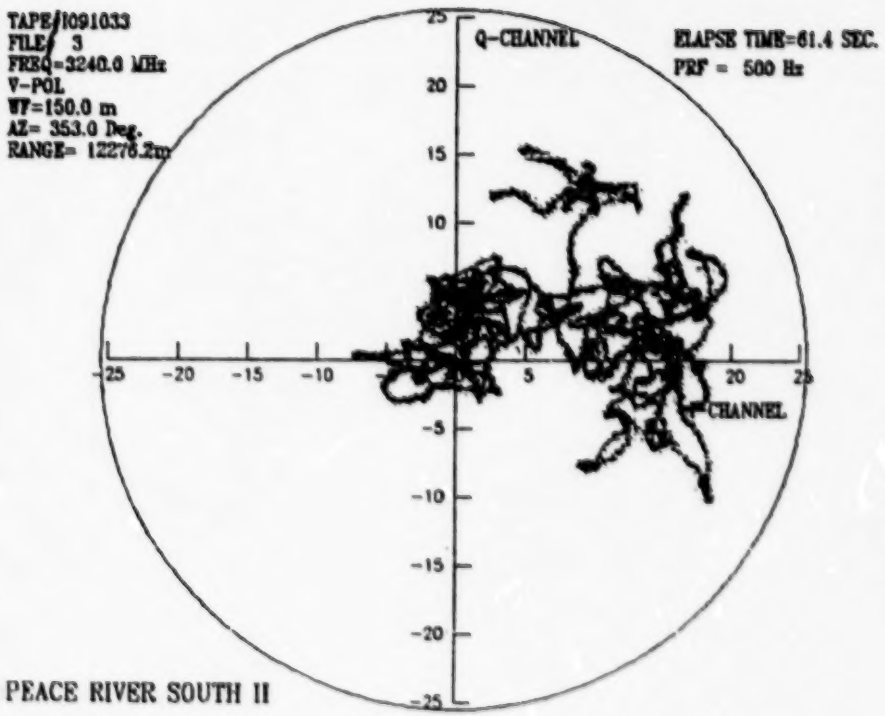

(a) Amplitude–phase scatter plot.

Figure 7. An example of nonstationary clutter processes.

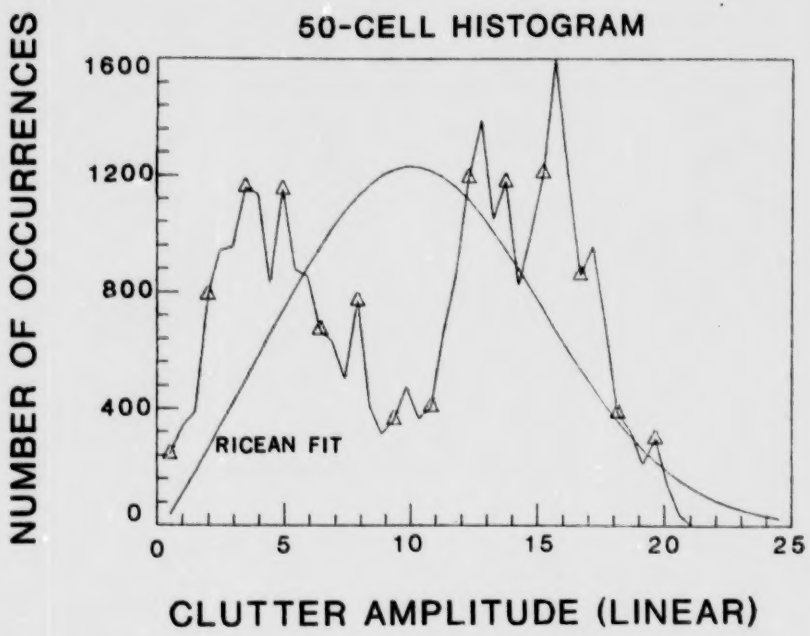

(b) Histogram.

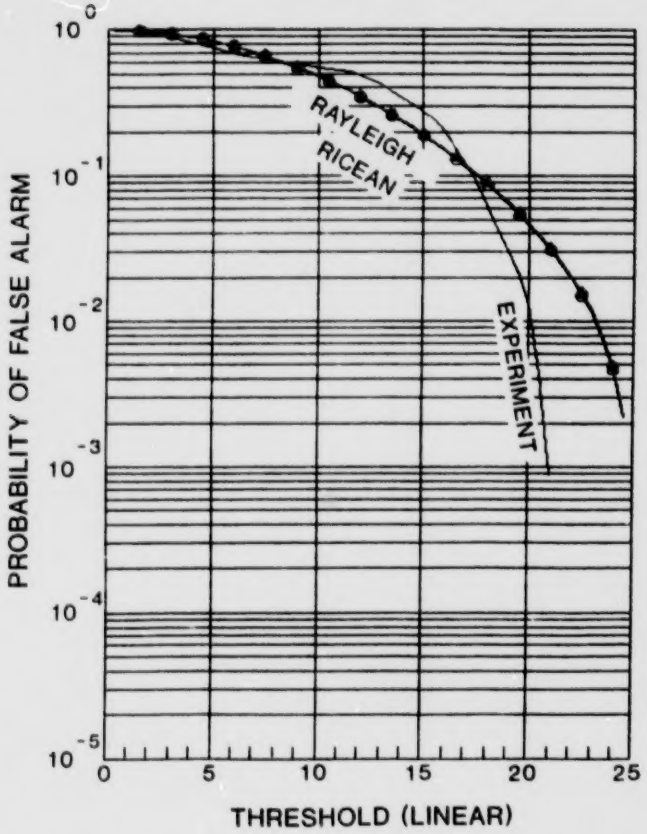

(c) Probability of false alarm.

Figure 7. An example of nonstationary clutter processes (Cont'd).

Table III tabulates the number of occurrences of fit to the two models for the Beiseker clutter data set (Table IIa). The recorded wind speed (w.s.) for each experiment is indicated. The result is divided into two parts: (i) for high–resolution experiments and (ii) for low–resolution experiments. Only the H–POL results are shown.

Table III: Classification of clutter amplitude statistics for the Beiseker (H–Pol) data.

	Low Resolution				High Resolution		
Band	w.s.	Rice.	Rayl.	Others	w.s.	Rice.	Rayl.	Others
X	7	10	5	1	7	28	48	0
S	7	13	3	0	12	32	44	0
L	7	10	6	0	7	46	30	0
UHF	7	14	2	0	7	45	3	0
VHF	7	16	0	0	5	35	41	0
		16 cells total				76 cells total		

Comparison of amplitude histograms of ground–clutter time–series for high (15m, 36m) and low (150m) resolution showed that there was a difference in the relative frequency of fit of the two models between the cases of high– and low–resolution waveforms. For example, a 150m range cell contains ten 15m cells. Some of these ten 15m cells may contain large stationary scatterers, while others may contain only small movable scatterers. As a result, clutter from cells containing only small scatterers would fit a Rayleigh model, while cells containing large scatterers would fit a Ricean model, when the 15m waveform resolution is used. On the other hand, a dominant steady scatterer in one of the 15m resolution cell will result in Ricean clutter amplitude statistics when the 150m waveform resolution was used.

Similarly the classification of clutter amplitude statistics for the Picture Butte data set is tabulated in Table IV. The land cover for the resolution cells from which these data were collected was classified as urban. No X–band data were collected at the Picture Butte site.

The Picture Butte result is interesting in two respects. First, we observed an increased number of resolution cells with clutter statistics deviating from those of the Ricean and the Rayleigh models compared to the Beiseker Results. This is attributed to the probable mixing of urban land cover with trees. It will be shown in Table V that forested land cover has a greater proportion of resolution cells with nonstationary clutter amplitude statistics.

Second, for VHF, we observed a greater proportion of the resolution cells with clutter having Rayleigh statistics. The random property of clutter is a consequence of the random cancellation and reinforcement of the returns from individual scatterers in the resolution cell. As the radar frequency decreases, the displacement of scatterers in terms of a fraction of the radar wavelength decreases. One therefore expects that a Ricean clutter process would be more probable. For Picture Butte at VHF, however, this was not the case for high resolution waveforms. By comparing the VHF data with those of other bands, we observed that the average clutter magnitudes were substantially lower at VHF. This led us to believe that multipath could have attenuated the normally large steady component, and as a result, the clutter statistics approached a Rayleigh process.

Table IV: Classification of clutter amplitude statistics for the Picture Butte data set (Table IIb).

	Low Resolution (V-POL)				High Resolution		
Band	w.s. (mph)	Rice.	Rayl.	Others	w.s. (mph)	Rice.	Rayl.	Others
S	15	13	0	3	15	46	27	3
L	11	12	0	4	11	58	17	1
UHF	10	16	0	0	10	66	10	0
VHF	7	11	5	0	7	10	66	0
		16 cells total				76 cells total		

	Low Resolution (H-POL)				High Resolution		
Band	w.s. (mph)	Rice.	Rayl.	Others	w.s. (mph)	Rice.	Rayl.	Others
S	16	10	2	4	16	48	26	2
L	11	15	0	1	15	42	33	1
UHF	7	15	0	1	7	60	14	2
VHF	7	12	4	0	7	9	67	0
		16 cells total				76 cells total		

The classification of clutter amplitude statistics for the Peace River South II data set is tabulated in Table V. The resolution cells from which these data were collected were classified as having deciduous forested land cover.

Table V: Classification of the clutter amplitude statistics for the Peace River South II data set (Table IIc).

	Low Resolution (V-POL)				High Resolution		
Band	w.s. (mph)	Rice.	Rayl.	Others	w.s. (mph)	Rice.	Rayl.	Others
X	5	8	7	1	5	37	28	11
S	2	8	2	6	2	50	19	7
L	8	10	4	2	8	44	20	12
UHF	8	9	0	7	8	59	0	17
VHF	5	16	0	0	1	76	0	0
	Low Resolution (H-POL)				High Resolution			
Band	w.s. (mph)	Rice.	Rayl.	Others	w.s. (mph)	Rice.	Rayl.	Others
X	5	8	7	1	5	30	41	5
S	2	7	5	4	2	26	43	7
L	8	8	2	6	8	49	10	17
UHF	8	10	0	6	2	65	0	11
VHF	1	16	0	0	1	74	0	2

The results obtained for Peace River South II (deciduous forest land cover) are quite different from those of Beiseker (agricultural land cover) and Picture Butte (urban land cover). We observed a significantly greater proportion of resolution cells with Rayleigh clutter statistics. As well, there were more resolution cells having nonstationary clutter statistics in comparison with the other two sites.

The results of the preceding tables suggested that, in most cases, temporal clutter statistics fit either the Ricean or the Rayleigh model. The goodness of fit is a function of radar frequency, wind speed, land cover and radar resolution. Polarization did not have any significant effect on the statistical behaviour of ground clutter. However, these results were obtained from a relatively small data base. In Section 3.2 we shall present results obtained from analyzing the larger DREO S–band ground–clutter data base.

3.2 Statistical classification of DREO clutter data

A large data base was available for S–band from the DREO S–band coherent phased–array radar. In this section, we compare three sets of S–band clutter time series recorded at progressively higher wind speeds. These data were recorded on separate days in February of 1989. The averaged wind speeds for the three sets of data were 3, 12 and 25 mph respectively.

There were 1200 resolution cells within the sector where the data were collected. Approximately half of these resolution cells were located on the Ottawa River. Data from these cells were excluded from the analysis since they represented mostly reflection from water. The remaining resolution cells were classified into three categories: type 1 – urban, type 2 – agricultural and type 4 – forested. Classification was done through interpretation of high resolution aerial photographs of the DREO site. Type 3 was designated as rangelands; however, there were no type 3 areas at the DREO site.

The urban land cover included residential and commercial buildings, highways, parking lots, terrain ridges and shore lines. The agricultural land cover included mostly fields with no visible trees but might include field boundaries and some farm buildings. The forested areas were primarily areas with trees. There were 108, 109 and 387 resolution cells classified as having urban, agricultural and forested land–covers, respectively.

The amplitude histograms of these sets of clutter data are classified against the Ricean and Rayleigh models, and the results are tabulated in Table VI.

Table VI: Classification of the clutter amplitude statistics for the DREO clutter data.

Land Cover	Wind Speed									Total No. of cells
	3 mph			12 mph			25 mph			
	Rice.	Rayl.	Others	Rice.	Rayl.	Others	Rice	Rayl.	Others	
1	63	0	45	40	9	59	35	23	41	108
2	78	3	28	43	28	38	24	45	40	109
4	238	4	145	175	92	120	94	185	108	387

These result show the effects of wind speed and land cover on clutter amplitude statistics. We observed that, for urban land cover (Land cover type 1), the majority of the resolution cells has clutter amplitude statistics approximately fitting the Ricean model. That is, for those resolution cells which had been classified as "others", the P_{fa} vs V_T curve is closer to the Ricean model than to the Rayleigh model, and the value of the parameter β is usually greater than 0.8. As the wind speed increased, the number of cells with Rayleigh and "nonstationary" amplitude statistics increased. Similar effects were observed for agricultural land covers (land cover type 2).

For forested land cover (land cover type 4), we observed a somewhat different result. The number of resolution cells classified as "others" actually decreased as the wind speed increased. In Section 3.3, we shall explore this result in more details.

3.3 Nonstationary clutter processes.

In compiling the results of the preceding tables, it was observed that there was a number of resolution cells with clutter data which did not fit well either the Rayleigh or the Ricean model. In this section, we shall examine these data more closely.

Detailed analysis of the histograms, P_{fa} vs V_T curves and the time–domain waveform of clutter data indicated that nonstationary clutter amplitude statistics belonged in one of two categories.

(i) The amplitude distribution is predominantly Ricean, and there is a short time interval in which the clutter statistics undergo changes, and

(ii) The amplitude distribution is predominantly Rayleigh, and there is a short time interval in which the clutter statistics undergo changes.

A Rayleigh process is the envelope of a zero–mean complex Gaussian process. Thus the I–channel and the Q–channel waveforms of a clutter process fitting the Rayleigh model will have frequent zero–crossings. A Ricean process, on the other hand, is characterized by a DC offset in either the I– or Q–component (or both). These characteristics may be used to categorize a clutter process from the clutter waveform.

Since wind is the most probable mechanism which causes movement of scatterers, these results support the hypothesis that nonstationary clutter amplitude statistics is a result of sudden changes in wind speed. An example of clutter data fitting category (i) is shown in Figure 8. In this figure we show the I–channel waveform of an L–band, V–POL experiment over a 60 second time interval. The DC offset of the waveform indicated that this clutter process was predominantly Ricean. There was, however, a period of about 12 seconds (pulses No. 9216 to No. 15360) in which the clutter behaved predominantly as a Rayleigh process, as evidenced by the increased number of zero–crossings in the waveform. The model parameters were derived from the first and second moments which were computed using the entire time series.

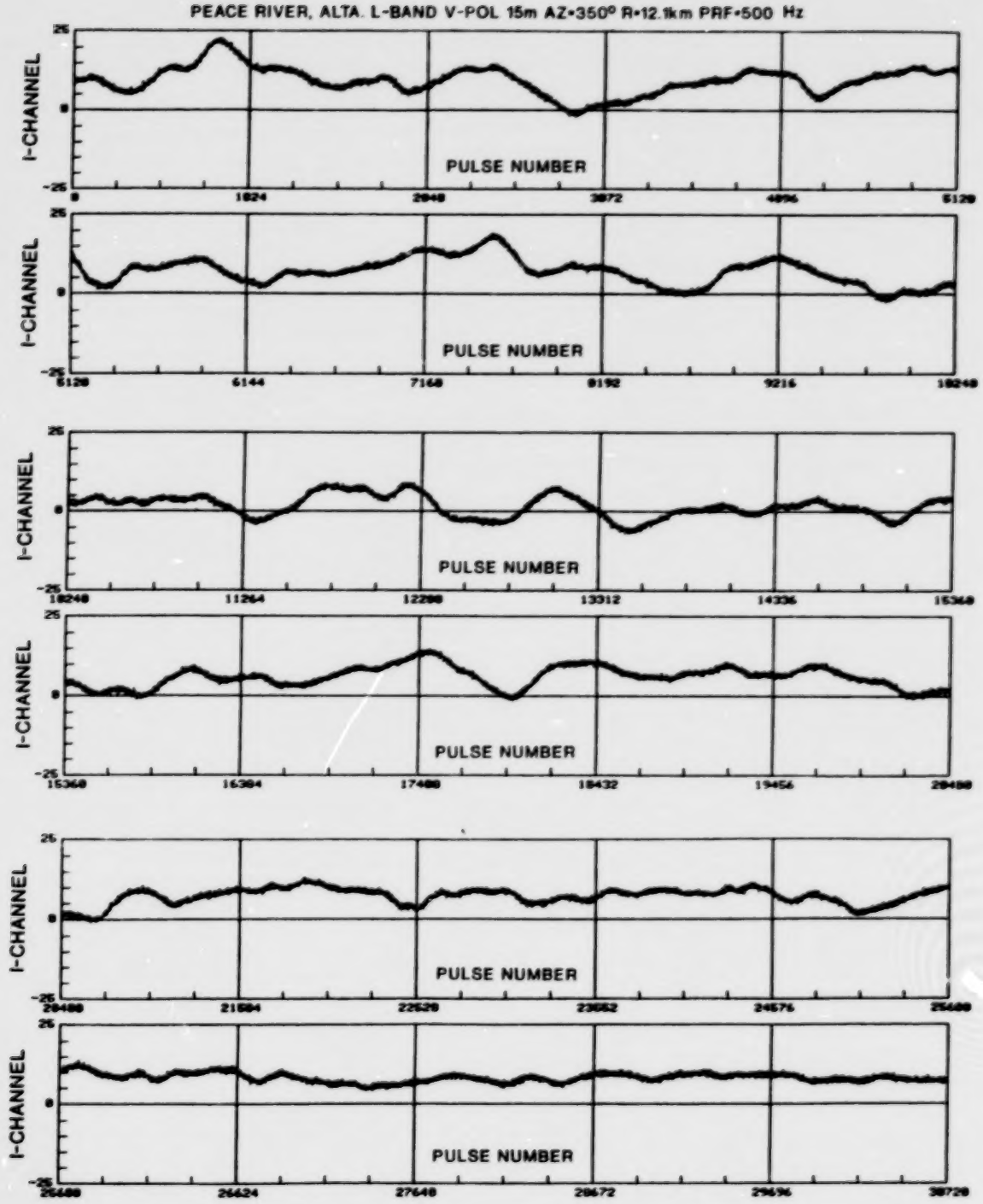

Figure 8. In-phase waveform of a nonstationary clutter process with a predominantly Ricean fit.

Since the clutter process illustrated in Figure 8 was predominantly Ricean, the P_{fa} behaviour generally followed the Ricean model except during the time interval in which the clutter statistics approached that of a Rayleigh model. Figure 9a shows the histogram and the theoretical pdf's of the Ricean and the Rayleigh model. The experimental histogram fitted the Ricean model better than the Rayleigh model. Figure 9b shows the corresponding P_{fa} vs V_T curves for the data, the Ricean and the Rayleigh models. The actual P_{fa} curve was bounded by those of the two models.

An example of clutter data fitting category (ii) is shown in Figure 10. In this figure we show the I–channel waveform of an L–band, H–POL experiment over a period of 60 seconds. For the first four seconds (pulses 0 to 2048) the clutter amplitude was substantially greater than that in the subsequent 56 seconds. The relatively frequent zero–crossings and the absence of a large DC offset in the waveform indicated that this clutter process was predominantly Rayleigh. In Figure 11a we show the histogram of the clutter data over the entire 60 second interval together with the Ricean and Rayleigh models computed from the first and second moments. The data fit the Rayleigh model slightly better than the Ricean model. However, there was a significantly longer tail in the experimental histogram compared to those of the models. In Figure 11b we show the P_{fa} vs V_T curves for the data, the Ricean and Rayleigh models. The actual false alarm probability was much higher than that predicted either by the Ricean or the Rayleigh model.

In Section 4.2 we will discuss possible ways to accommodate nonstationary clutter amplitude distributions in regard to constant false alarm regulation. We have introduced the parameter β in Section 2.3. This parameter can be used as a means to classify clutter process in each of the resolution cell. For a Ricean process (referring to Eqns (4) and (5)), the value of β lies between $\pi/4$ and unity, corresponding to the limiting cases of $A^2/2\sigma^2=0$ and $A^2/2\sigma^2=\infty$, respectively. To get some indication of how often the ground clutter statistics fit the two models in a typical site such as the one at DREO, we plotted the values of β as a function of resolution cell number for each land cover type. The numbering of the resolution cell is arbitrary. For example, there were 108 resolution cells in the DREO data which were classified as having urban land covers. We assigned a number to each of these resolution cells ranging from 0 to 107. A similar numbering scheme was used for agricultural and forested land covers.

Figure 12 shows the value of β as a function of resolution cell number for land cover type 1 (urban) at the DREO site for three different wind speeds. At an averaged wind speed of 3 mph, the majority of the 108 resolution cells have a value of β close to unity. This indicates that most of the resolution cells in an urban area had clutter that was predominantly Ricean. At an averaged wind speed of 12 mph, a number of the resolution cells had β values less than 0.9, and some even approached the Rayleigh limit of $\pi/4$. However, for the majority of the resolution cells, the Ricean distribution was the best model. At an averaged wind speed of 25 mph, a slightly increased number of resolution cells with predominantly Rayleigh statistics was observed.

Figure 13 shows the value of β as a function of resolution cell number for land cover type 2 (agricultural). At low wind speeds, the majority of the resolution cells had clutter that was predominantly Ricean. At higher wind speeds, the majority of the resolution cells had clutter that was predominantly Rayleigh.

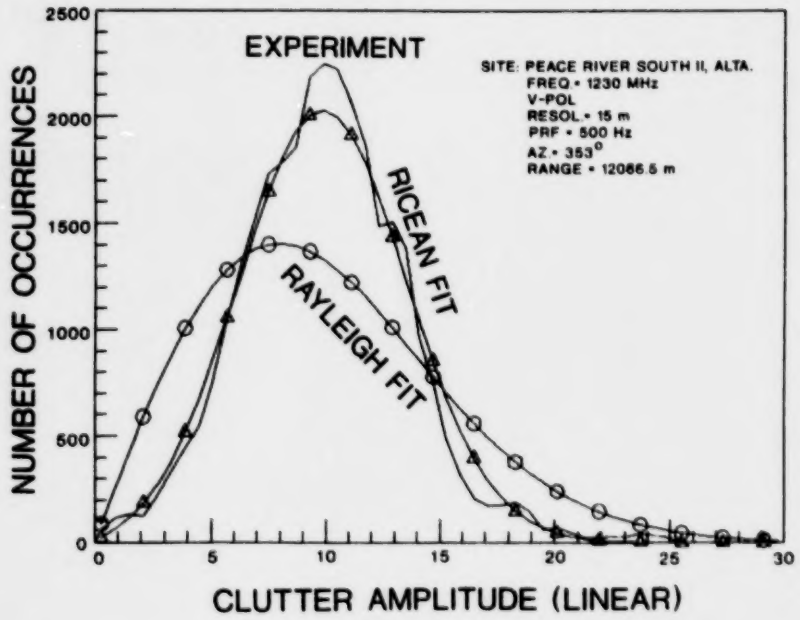

(a) Histogram

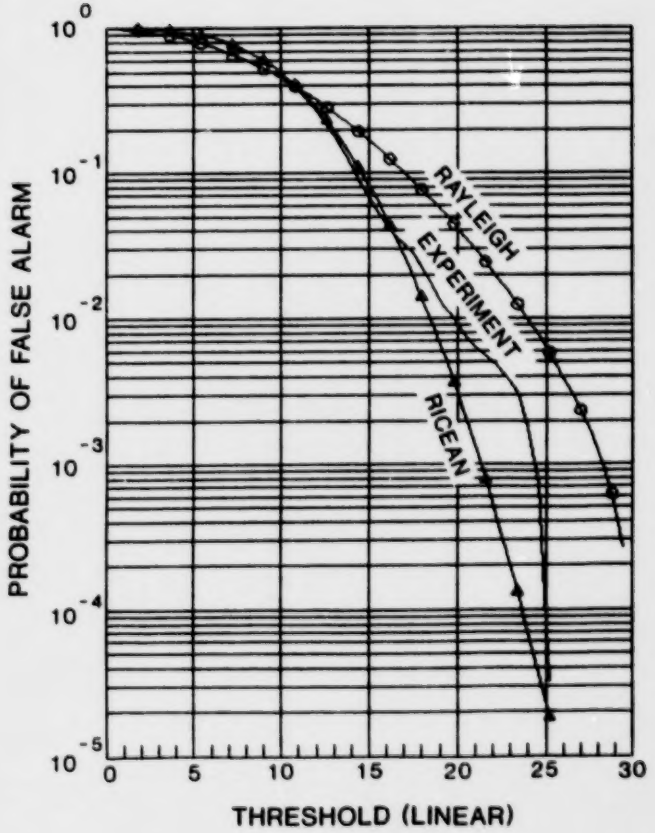

(b) Probability of false alarm.

Figure 9. An example of nonstationary clutter processes with a predominantly Ricean fit.

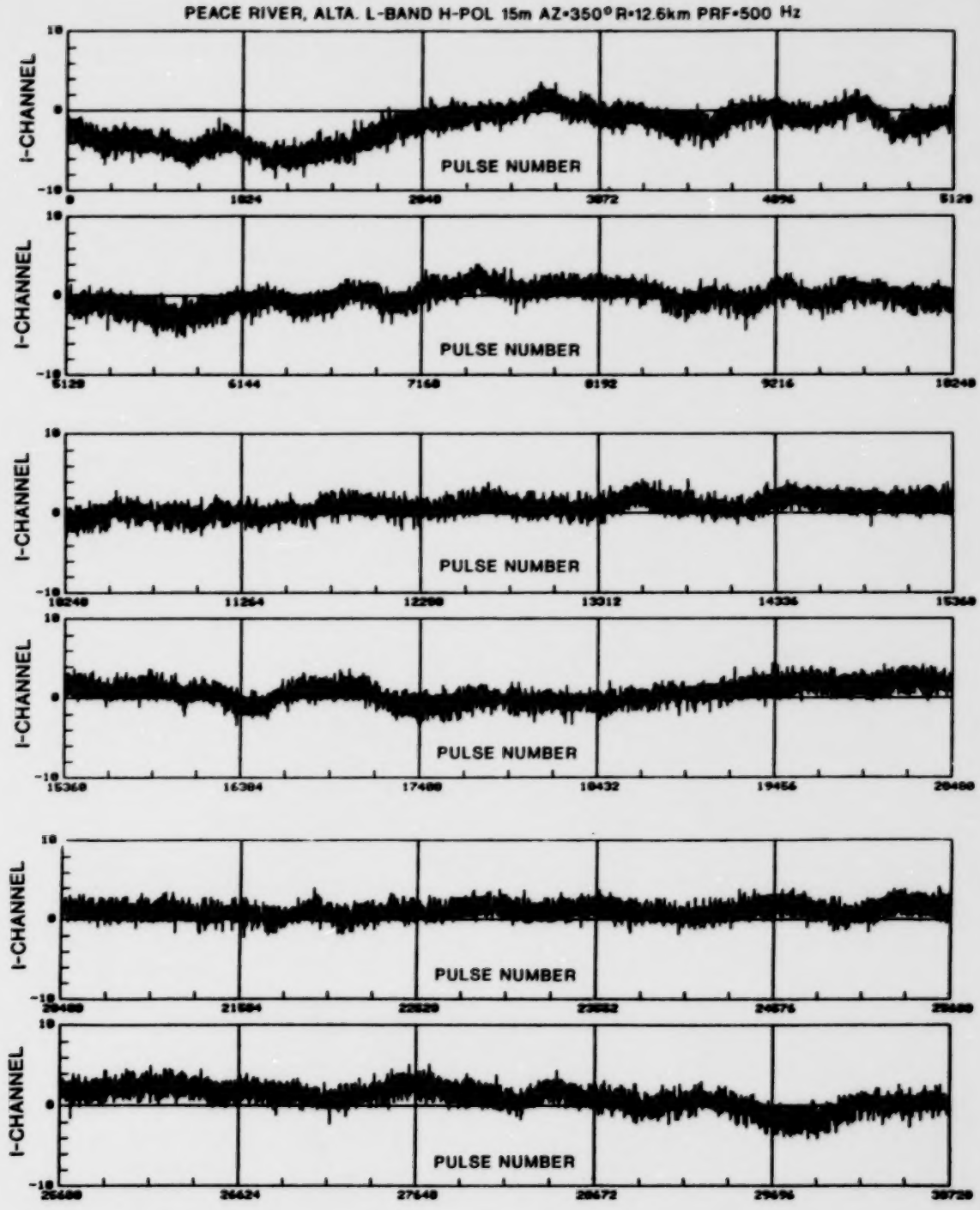

Figure 10. In-phase waveform of a nonstationary clutter process with a predominantly Rayleigh fit.

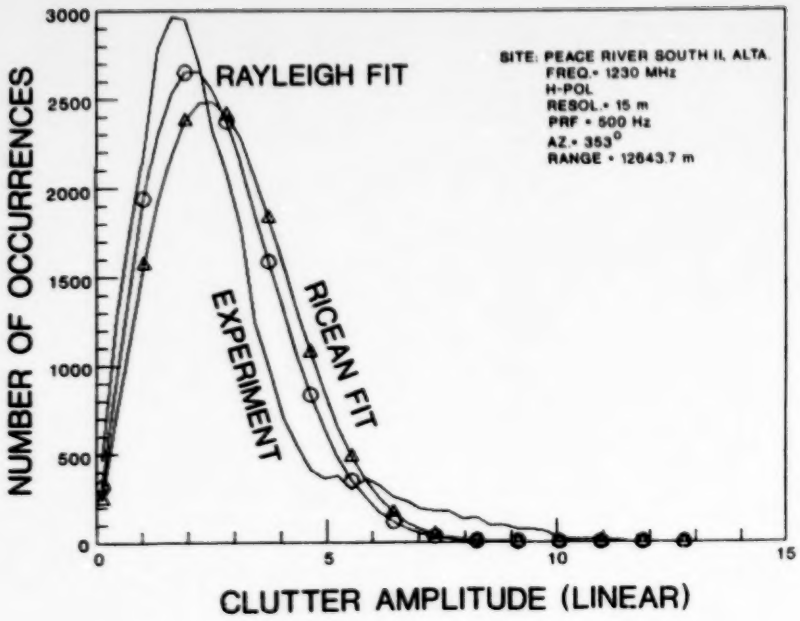

(a) Histogram

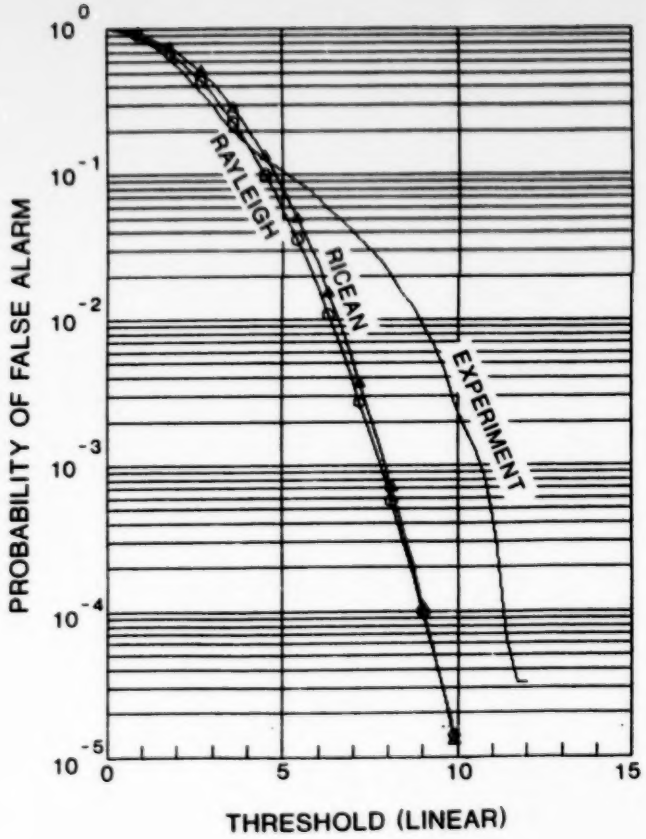

(b) Probability of false alarm.

Figure 11. An example of nonstationary clutter processes with a predominantly Rayleigh fit.

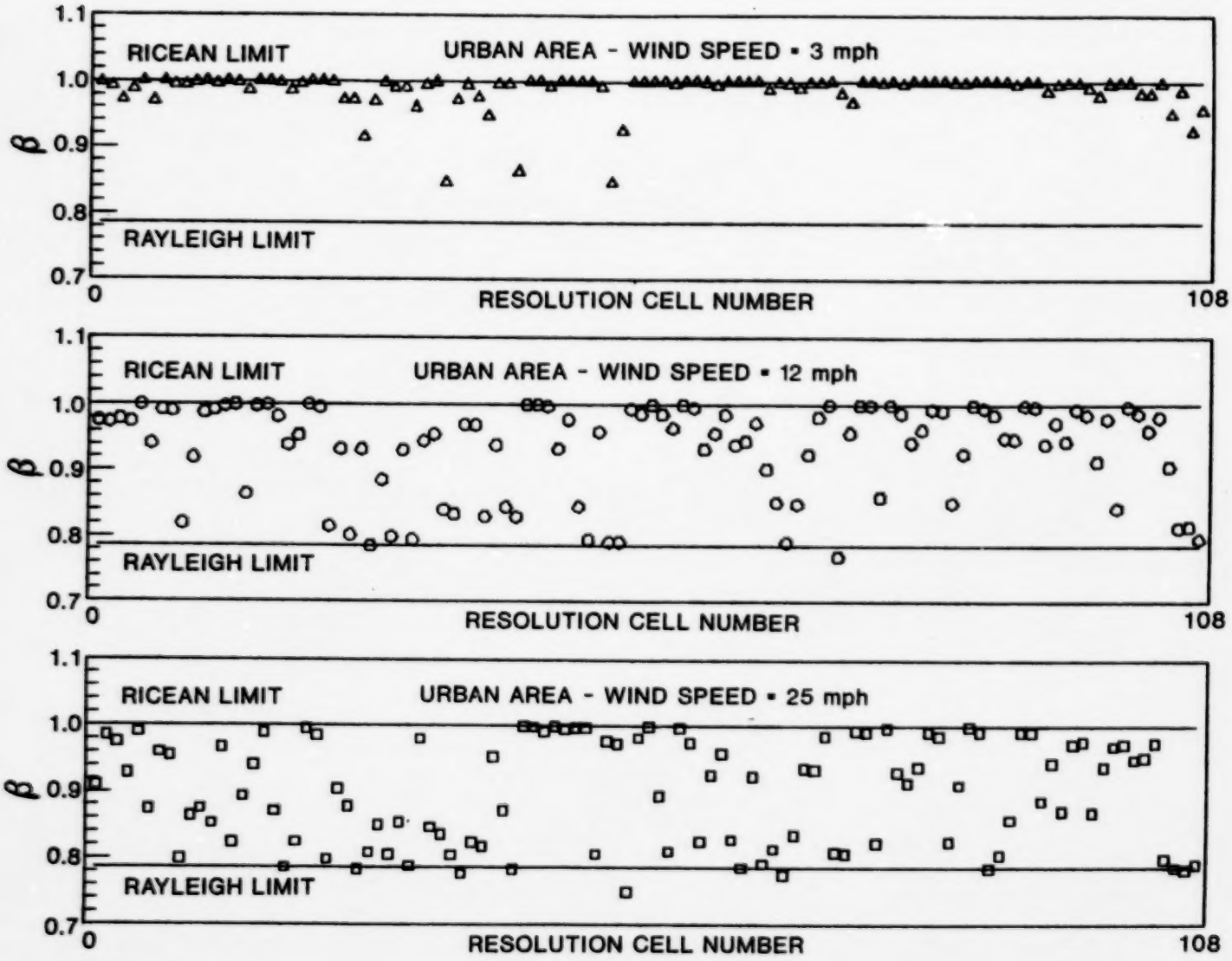

Figure 12. Distribution of parameter β for clutter in urban areas at the DREO site.

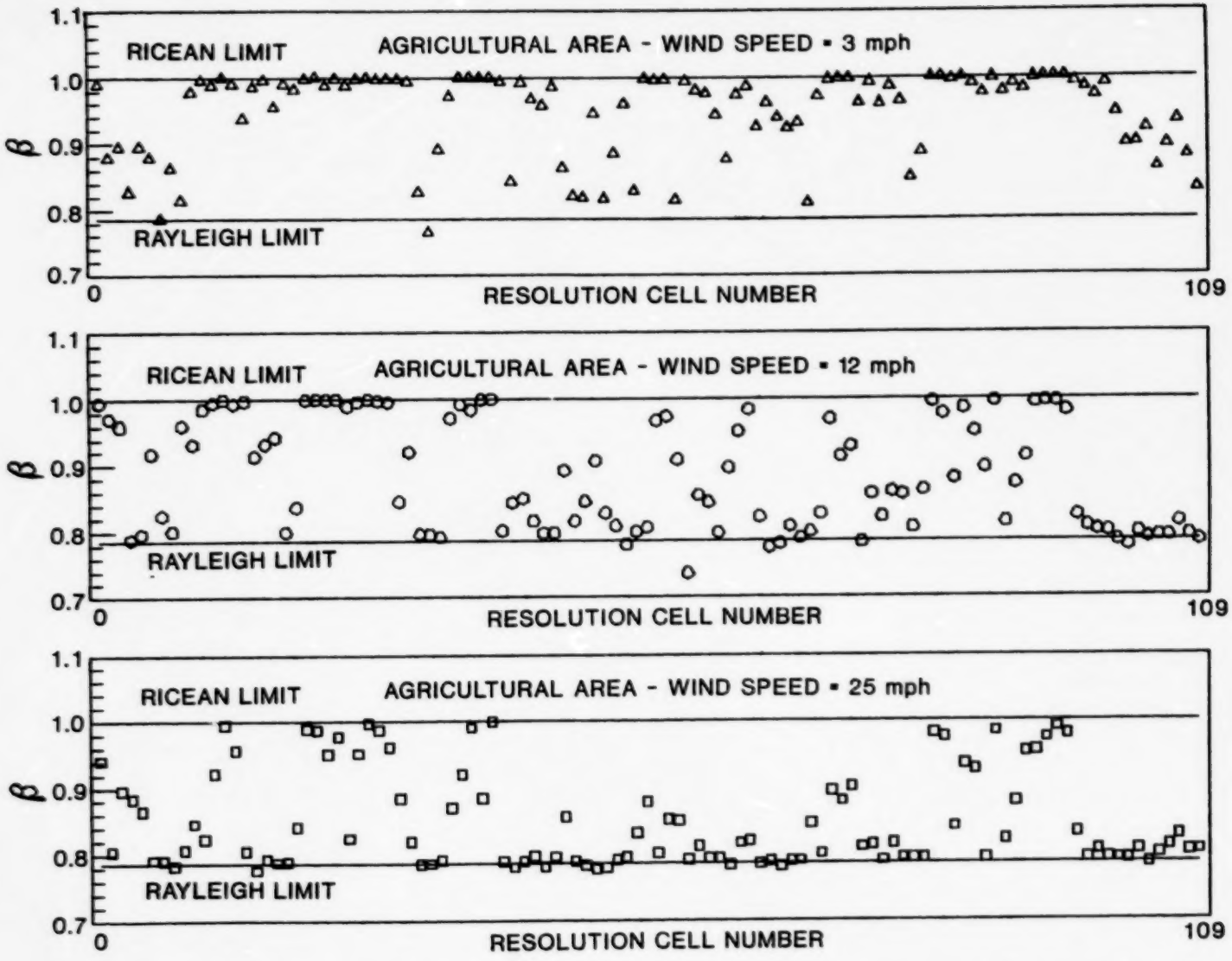

Figure 13. Distribution of parameter β for clutter in agricultural areas at the DREO site.

Significantly different results were observed for forested land covers. Figure 14 shows the value of β as a function of resolution cell number for type 4 (forested) land cover. At low averaged wind speeds, most of the resolution cells had clutter that could be classified as predominantly Ricean. However, there were still many resolution cells with a β value below 0.95 which indicated that the coherent–to–diffuse component ratio was low. At moderate averaged wind speeds, the number of resolution cells with β values close to unity decreased drastically, indicating that the clutter in more resolution cells was becoming incoherent. At high wind speeds (25 mph), most of the resolution cells had β values close to $\pi/4$, indicating that the distribution function for clutter in most of the resolution cells could be appropriately modelled as a Rayleigh process.

4. Conclusions

In this study, we carried out a detailed analysis of low–angle ground clutter to characterize its temporal amplitude statistics. The analysis was performed using data collected by the MIT Lincoln Laboratory at several western Canadian sites as well as data from the DREO site. The variation of the site environment at the time of data recording enable us to extract information with regard to the effect of wind speed and land covers on the observed amplitude statistics. The results confirmed the theoretical conjecture that the Ricean distribution is an appropriate model for describing the temporal amplitude statistics of ground clutter. However, there was a significant portion of the total resolution cells in a surveillance area with nonstationary temporal statistics. The main findings of this study are summarized in Section 4.1.

4.1 Summary of results

(i) The temporal statistics of ground clutter are best modelled by a Ricean distribution which sometimes degenerated into a Rayleigh distribution. The relative frequency of occurrence of fit of clutter data to the two models is a function of land cover, wind speed, radar frequency and resolution;

(ii) At any given time, there was a fraction of the resolution cells in a surveillance area whose clutter amplitude exhibits some degree of nonstationarity. Occurrence of nonstationary statistical behaviour is more likely in forested areas;

(iii) Histograms of clutter from forested areas generally had poor visual resemblance to the theoretical pdf's. However, the actual P_{fa} vs V_T curve was bounded above and below by those of the Rayleigh and the Ricean models, respectively;

(iv) Nonstationary statistical behaviour of clutter amplitude was most likely the results of sudden changes in wind velocity.

(v) Four parameters, radar frequency, waveform resolution, land cover and wind speed influenced temporal clutter statistics.

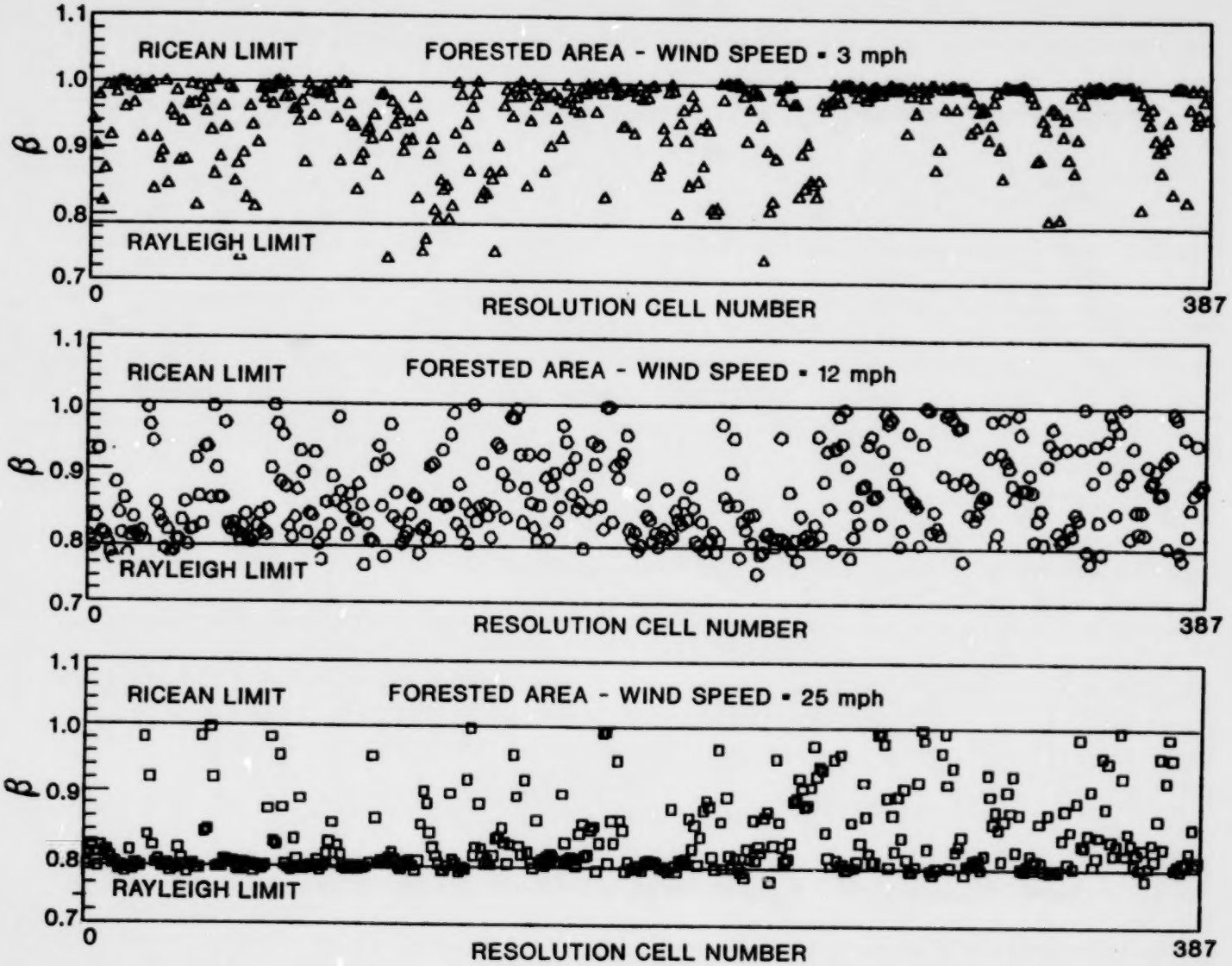

Figure 14. Distribution of parameter β for clutter in forested areas at the DREO site.

(a) Radar frequency

Radar frequency influences the temporal statistical behaviour of ground clutter in wind because the physical displacement of the scatterers, as measured in wavelengths, is a function of frequency. At X–band, the wavelength is about 3 cm, whereas at VHF, it is almost two meters. The diffuse clutter component caused by the random reinforcement and the cancellation of radar returns due to the relative displacement of scatterers may be very large at X– and S–bands but generally would be much smaller at VHF. As a result, a clutter process may exhibit Rayleigh behaviour at X–band but Ricean behaviour at UHF and VHF.

In addition, radar frequency could influence the temporal statistics of ground clutter through multipath. Multipath phenomenon is more prevalent at low frequencies for low angle ground clutter. A Ricean clutter process comprises a large steady component and a diffuse component. Cancellation of the steady component by multipath would result in a Rayleigh process even if there exists a large scatterer in a resolution cell.

(b) Waveform resolution

With a high resolution waveform, the location of dominant scatterers can be isolated, thereby causing the clutter from resolution cells with mainly small movable scatterers to have a Rayleigh density and those with isolated large scatterers to have a strongly Ricean density.

(c) Land covers

The type of land cover has a strong influence on the temporal statistical behaviour of ground clutter.

Urban land cover

For urban land cover, the scatterers are mostly man–made objects such as residential and commercial buildings, highways, parking lots, etc. The probability of having a large steady scatterer in a resolution cell is very high. Consequently, the occurrence of a strongly Ricean clutter amplitude distribution is more frequent than for any other land covers.

As noted in Section 3, clutter with nonstationary statistics occurred more often in forested terrains. To the extent that urban areas might include a fair number of trees (e.g., most residential house may have a few trees nearby), there could also be a significant portion of resolution cells with nonstationary clutter–amplitude statistics. However, in this case, the steady or coherent component due to returns from buildings still dominates, and the clutter process are usually strongly Ricean.

Agricultural land cover

We considered an area with agricultural land cover to be one with homogeneous vegetation. There could be field boundaries, roads and isolated farm houses which are steady scatterers. Crops in the fields are diffuse scatterers. Returns from crops are weaker than those from trees. As a result, clutter from an agricultural area should exhibit a moderate or strongly Ricean amplitude distribution.

Forested land cover

The dominant scatterers in a forested area are trees. Tree leaves and branches constitute a majority of the visible part of a tree. Thus the entire ensemble of scatterers may be considered movable. The magnitude of the diffuse component is large compared to the steady component (e.g., reflection from tree trunks). As a result, the occurrence of weakly Rayleigh amplitude distribution is more probable in a forested area.

Tree leaves and branches have different masses. Tree leaves are more easily set into steady state motion by relatively light wind, while tree branches require a substantially higher wind speed to attain a steady oscillatory motion. If there is a sudden change in wind speed, such as that of a wind gust, the motion of the branches would be drastically different. Since there are numerous leaves attached to a branches, we have a situation wherein the motions of light scatterers (those of the leaves) are modulated by a different random motion (that of the tree branches). This is likely why nonstationary clutter–amplitude behaviour was observed more often in forested terrains.

(d) Wind speed

Wind speed is another parameter which has a direct influence on ground clutter temporal statistics. Theoretically, if there were no wind and everything were to remain motionless, the clutter amplitude statistics would be Ricean, because the receiver noise is Gaussian. At low wind speeds, the light scatterers are set in motion. Experimental evidence shows that the distribution of clutter amplitude under this condition is Ricean. As the wind speed increases, more and more scatterers are set in motion. Depending on the relative proportion of movable and immovable scatterers, the clutter–amplitude statistics could approach a Rayleigh distribution. As noted before, nonstationary clutter–amplitude statistics are the result of sudden wind speed changes.

4.2 Constant false–alarm rate considerations.

Modern radars employ some form of signal processing of a varying degree of sophistication to combat the effect of ground clutter. The simplest form is the Moving Target Indicator (MTI) filter such as a two–pulse canceler. More sophisticated system such as the Moving Target Detector (MTD) [7] employed a bank of band–pass filters, each optimized for target–to–noise ratio and target–to–clutter ratio. In most cases (except at higher frequencies, say X–band, and at high wind speeds), the clutter spectrum will be entirely within the passband of the zero–velocity filter (ZVF). Targets having a Doppler within the passband of the ZVF must compete with a large clutter component. It is essential to know the amplitude distribution of the clutter at the output of the ZVF so as to minimize loss of detectability for low–velocity targets due to non–optimum settings of the detection threshold.

4.2.1 Optimal detection threshold settings.

In a MTD processor, a non coherent map of the clutter magnitude for each resolution cell within the surveillance area is maintained to provide a means of setting the detection threshold. Since the non coherent clutter map provides only the estimate of the mean, to obtain the threshold setting for a given probability of false alarm, a Rayleigh clutter amplitude (or an exponential power) distribution is assumed. This is not very satisfactory for many cases (e.g., a radar operating in very low wind speed conditions, in urban areas, or at low radar frequencies). The quantity $A^2/2\sigma^2$ represents the ratio between the coherent and the diffuse spectral power of ground clutter. Ground clutter will be more coherent when $A^2/2\sigma^2 >> 1$ (β approaches unity). In Table VII we compared the detection threshold settings estimated from (a) the Rayleigh model, and (b) the Ricean model, for a P_{fa} of 10^{-6}. Unity σ was assumed.

Table VII. Threshold settings for the Rayleigh and Ricean Models

$A^2/2\sigma^2$ (dB)	Coherent Component Amplitude	1st moment (Ricean)	2nd Moment (Ricean)	β	Rayleigh V_T @$P_{fa}=10^{-6}$	Ricean V_T @$P_{fa}=10^{-6}$
$-\infty$	0.	1.253	2	$\pi/4$	5.2565	5.2565
0	1.414	2.272	6	0.8606	11.9448	6.3225
10	4.472	4.585	22	0.9557	24.1036	9.3017
20	14.142	14.177	202	0.9951	74.5243	18.9260
30	44.721	44.732	2002	0.9995	235.1347	49.4854

The above comparison demonstrates a need to optimize the detection threshold settings. For a completely diffuse clutter process, (i.e, A=0), Eqn (4) reduces to Eqn (7) and the Ricean mean and the Rayleigh mean are identical. Consequently, the P_{fa} for the two models are identical. As the coherent clutter component increases ($A^2/2\sigma^2>>1$), the P_{fa} vs V_T behaviour of the two models begins to differ. Generally, if the clutter statistics are moderately to strongly Ricean, the threshold level required for a given P_{fa} is substantially lower than the one computed from the Rayleigh model. In Section 3.3 we used the parameter β as a discriminant to indicate whether a clutter process is strongly Ricean or strongly Rayleigh. To classify ground clutter adequately, we need an estimate of the first and second moments from which we can calculate β. From β, we can obtain the appropriate threshold setting which can be obtained from a look–up table. This process is no more complicated than that used in existing systems using clutter maps. The non–coherent clutter map then stores the appropriate value of threshold setting, V_T, which is updated every time β is updated.

4.2.2 Detection threshold for nonstationary clutter process.

In section 3.3, we observed that clutter which exhibited nonstationary amplitude statistics belonged to one of two categories, (i) predominantly Ricean and (ii) predominantly Rayleigh. We observed further that for type (i), the actual P_{fa} curves were bounded above by the Rayleigh P_{fa} curve. For type (ii), the actual P_{fa} curve could exceed that predicted by the Rayleigh model.

Intuitively, one would expect that these should be the cases for the following reasons. First, for a predominantly Ricean clutter process, there is a finite coherent component A. Hence the P_{fa} characteristic will be below that calculated by assuming a zero coherent component (A=0, Rayleigh model). The actual P_{fa} characteristic of the clutter may deviates from that of a model because of (a) inaccuracy in the model parameter estimation and (b) nonstationary statistical behaviour. A nonstationary clutter behaviour will result either in it being more coherent (increasing A) or it being more incoherent (decreasing A). For a clutter process becoming more incoherent, one expects a P_{fa} characteristic to approach that calculated by assuming a Rayleigh model.

Second, for clutter data from resolution cells with a value of β very close to $\pi/4$, the coherent component A is nearly zero. Consequently, the P_{fa} characteristics calculated by assuming a Ricean and Rayleigh models are very close to each other. A change in the clutter statistics could result in the P_{fa} characteristic exceeding both of those calculated from the Ricean and the Rayleigh models.

For optimal false alarm regulation and maximum detection performance, the detection threshold should be determined using the Ricean model, with a multiplying factor to accommodate nonstationary statistical behaviour. This multiplying factor is normally slightly greater than unity. The exact value, however, must be determined experimentally for various land covers, wind speeds and radar frequencies. More research is needed to determine the exact boundaries for various cases. Nevertheless, it is clear that substantial improvement in detection performance for low–Doppler targets can be realized if the knowledge of the temporal statistics of ground clutter is incorporated.

5. References

[1] Billingsley, J.B., "Phase One Master Directory File", MIT Lincoln Laboratory CMDT Project Memorandum No.45 PM–CMT–0003, September 1985.

[2] Rice, S.O., "The Mathematical Analysis of Random Noise", Bell System Technical Journal, vol.23, pp282–332, July 1944.

[3] Papoulis, A., "Probability, Random Variables and Stochastic Process", McGraw–Hill Book Company, New York, New York, 1965.

[4] Beckett, R. and Hurt, J. "Numerical Calculations and Algorithms", McGraw–Hill Series in Information and Computer, McGraw–Hill Book Company, New York, 1967.

[5] Smirnov, N., "Table for Estimating the goodness of fit of Empirical Distributions", Annal of Mathematical Statistics, vol.19, pp.279–281, 1948.

[6] Guttman, I., "Introductory Engineering Statistics", John Wiley and Sons, Inc., New York, New York, 1965.

[7] Karp, D. and Anderson, J.R., "Moving Target Detector (Mod. II) Summary Report", MIT Lincoln Laboratory Report No. ATC–95, November 1981.

6. Acknowledgement

The author thanks the U.S. Defence Advanced Research Projects Agency and the personnel of Group 45 of the MIT Lincoln Laboratory for furnishing the clutter data used in this study. Special thanks are due Dr. R.M. Turner for useful discussions on parameter estimation and for reviewing of the manuscript.

DOCUMENT CONTROL DATA

(Security classification of title, body of abstract and indexing annotation must be entered when the overall document is classified)

1. ORIGINATOR (the name and address of the organization preparing the document. Organizations for whom the document was prepared, e.g. Establishment sponsoring a contractor's report, or tasking agency, are entered in section 8.)

DEFENCE RESEARCH ESTABLISHMENT OTTAWA

2. SECURITY CLASSIFICATION (overall security classification of the document. including special warning terms if applicable)

UNCLASSIFIED

3. TITLE (the complete document title as indicated on the title page. Its classification should be indicated by the appropriate abbreviation (S,C,R or U) in parentheses after the title.)

TEMPORAL STATISTICS OF LOW-ANGLE GROUND CLUTTER (U)

4. AUTHORS (Last name, first name, middle initial)

CHAN, HING C.

5. DATE OF PUBLICATION (month and year of publication of document)

DECEMBER 1989

6a. NO. OF PAGES (total containing information. Include Annexes, Appendices, etc.)

43

6b. NO. OF REFS (total cited in document)

7

7. DESCRIPTIVE NOTES (the category of the document, e.g. technical report, technical note or memorandum. If appropriate, enter the type of report, e.g. interim, progress, summary, annual or final. Give the inclusive dates when a specific reporting period is covered.)

TECHNICAL REPORT

8. SPONSORING ACTIVITY (the name of the department project office or laboratory sponsoring the research and development. Include the address.)

DEFENCE RESEARCH ESTABLISHMENT OTTAWA, 3701 CARLING AVENUE, OTTAWA, ONTARIO, K1A 0Z4

9a. PROJECT OR GRANT NO. (if appropriate, the applicable research and development project or grant number under which the document was written. Please specify whether project or grant)

041LC12

9b. CONTRACT NO. (if appropriate, the applicable number under which the document was written)

10a. ORIGINATOR'S DOCUMENT NUMBER (the official document number by which the document is identified by the originating activity. This number must be unique to this document.)

DREO REPORT No. 1021

10b. OTHER DOCUMENT NOS. (Any other numbers which may be assigned this document either by the originator or by the sponsor)

11. DOCUMENT AVAILABILITY (any limitations on further dissemination of the document, other than those imposed by security classification)

(X) Unlimited distribution
( ) Distribution limited to defence departments and defence contractors; further distribution only as approved
( ) Distribution limited to defence departments and Canadian defence contractors; further distribution only as approved
( ) Distribution limited to government departments and agencies; further distribution only as approved
( ) Distribution limited to defence departments; further distribution only as approved
( ) Other (please specify):

12. DOCUMENT ANNOUNCEMENT (any limitation to the bibliographic announcement of this document. This will normally correspond to the Document Availabilty (11). However, where further distribution (beyond the audience specified in 11) is possible, a wider announcement audience may be selected.)

UNLIMITED

UNCLASSIFIED

SECURITY CLASSIFICATION OF FORM

13. ABSTRACT (a brief and factual summary of the document. It may also appear elsewhere in the body of the document itself. It is highly desirable that the abstract of classified documents be unclassified. Each paragraph of the abstract shall begin with an indication of the security classification of the information in the paragraph (unless the document itself is unclassified) represented as (S), (C), (R), or (U). It is not necessary to include here abstracts in both offical languages unless the text is bilingual).

Detailed knowledge of the temporal statistics of ground clutter is essential to determine the detection threshold settings so as to maximize the probability of target detection while maintaining an acceptable probability of false alarm. The performance of existing false alarm control schemes is often limited due to a lack of detailed knowledge of the ground-clutter temporal statistics. In this study, we analyze experimental data to characterize the temporal statistics of low-angle ground clutter in terms of the clutter's linear amplitude distribution. Effects of radar frequency, polarization, waveform resolution, land covers and wind speed on the statistics are examined.

The results show that the Ricean distribution and its limiting case, the Rayleigh distribution, are appropriate models for ground clutter in steady-state wind conditions. This implies that the diffuse clutter components, which give rise to the random properties of ground clutter, may be modelled as a complex Gaussian process. We found, however, that at any given time, there is a fraction of the resolution cells with clutter data having nonstationary temporal statistics not well modelled by the Ricean or Rayleigh distribution. The frequency of occurrence of nonstationary clutter statistics depends on radar frequency, land cover and wind speed. Forested land cover represents the worst case scenario. Application of the results of this study to determine optimal detection threshold settings is discussed.

14. KEYWORDS, DESCRIPTORS or IDENTIFIERS (technically meaningful terms or short phrases that characterize a document and could be helpful in cataloguing the document. They should be selected so that no security classification is required. Identifiers, such as equipment model designation, trade name, military project code name, geographic location may also be included. If possible keywords should be selected from a published thesaurus, e.g. Thesaurus of Engineering and Scientific Terms (TEST) and that thesaurus-identified. If it is not possible to select indexing terms which are Unclassified, the classification of each should be indicated as with the title.)

RADAR, GROUND CLUTTER, AMPLITUDE STATISTICS, CLUTTER MODEL, FALSE ALARM RATE